DEPARTMENT OF THE AIR FORCE

AIR UNIVERSITY (ATC)

AIR FORCE INSTITUTE OF TECHNOLOGY

Wright-Patterson Air Force Base, Ohio

AFIT/GNE/PH/83M-9

THREE-TEMPERATURE HOMOGENEOUS MODEL OF THE RADIATIVE GROWTH PHASE OF A FREE AIR NUCLEAR FIREBALL

THESIS

AFIT/GNE/PH/83M-9

Kirk A. Mathews
LCDR USN

AFIT/GNE/PH/83M-9

THREE-TEMPERATURE HOMOGENEOUS MODEL OF THE RADIATIVE GROWTH PHASE OF A FREE AIR NUCLEAR FIREBALL

THESIS

Presented to the Faculty of the School of Engineering
of the Air Force Institute of Technology
Air University
in Partial Fulfillment of the
Requirements for the Degree of
Master of Science

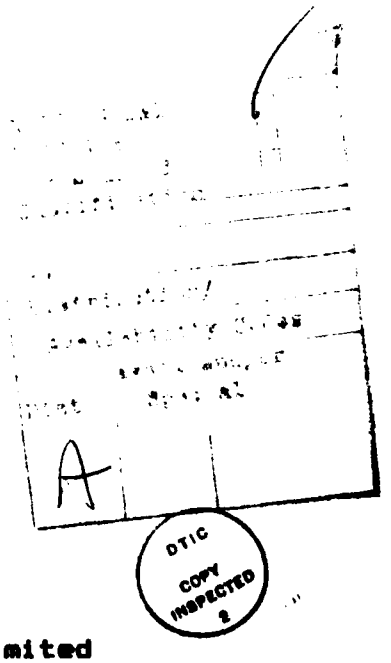

by

Kirk A. Mathews, B.S.
LCDR USN
Graduate Nuclear Engineering

December 1982

Acknowledgments

I would like to thank my faculty advisor, Dr. Charles Bridgman, for his advice and encouragement and for bringing Dr. Pomraning's work to my attention. Professor Bridgman's acceptance of this thesis topic in response to my interest in the problem, and the free reins he gave me once the problem had been formulated, are both greatly appreciated.

Contents

Contents

Contents

List of Figures

List of Tables

List of Symbols

Symbol	Value	Units	Interpretation
A		m^2	Surface area of fireball
a	13.7	$J/m^3/eV^4$	Radiation constant
b	0.0892	$shake^{-1}$	Energy conversion coefficient: $\rho \propto K^{(T_b)}$
C(T)		$shake^{-1}$	Energy conversion coefficient: $\rho \propto K^{(T)}$
C_1	$3.13*10^{10}$	$J/m^3/sh$	Emission rate of thermal radiation at burnout
c	3.00	m/shake	Speed of light
c_v	$1.24*10^{8}$	$J/m^3/eV$	Heat capacity of sea level air
dE_{mt}		J/m^3	Increment of energy density transferred from material to thermal radiation
dE_{sm}		J/m^3	Increment of energy density transferred from streaming radiation to material
E_b	$4.96*10^{10}$	J/m^3	Material energy density of sea level air at burnout
E_m		J/m^3	Energy density of material (air)
E_s		J/m^3	Energy density of streaming radiation
E_t		J/m_3	Energy density of thermal radiation
f(t)		$shake^{-1}$	Normalized yield rate: (dY/dt) / Y
F		J/m^3	Retarded time integral
G		$sh-J/m^3$	Retarded time integral
H		sh^2-J/m^3	Retarded time integral

List of Symbols

Symbol	Value	Units	Interpretation
I		shake	Retarded time integral
R		m	Radius of fireball
S		$J/m^3/sh$	Net source rate of E_t (emission - absorption)
T_b	400	eV	Temperature of air at burnout
T_{eff}		eV	Thermal radiation "effective" (blackbody equivalent) temperature
T_m		eV	Material Temperature
T_s		eV	Source (Device) Temperature
t		shake (= 10^{-8} sec)	Time
t'		shake	Retarded time of streaming radiation at fireball surface
t_{max}		shake	Time of peak of exponential form of f(t)
Y		kiloton	Yield (x-ray)
α		$shake^{-1}$	shape parameter in exponential form of f(t)
β		$shake^{-1}$	shape parameter in exponential form of f(t)
η		none	Attenuation factor in recursion relation for I(t)
κ		m^2/Kg	Opacity of sea level air
κ_s		m^2/Kg	Opacity of fireball to streaming radiation
κ_t		m^2/Kg	Opacity to thermal radiation
κ_b	0.023	m^2/Kg	Opacity of sea level air at burnout temperature

List of Symbols

Symbol	Value	Units	Interpretation
λ	50	m	Photon mean free path in sea level air at burnout
ρ	1.293	Kg/m^3	Density of sea level air
τ		shake	Retarded time variable of integration

Abstract

A model is developed which treats the growth of a fireball from an atmospheric nuclear detonation up to the point of hydrodynamic separation. The radius of the fireball and the partition of energy among streaming radiation, material temperature, and thermal radiation are predicted as a function of time. A simplified model is developed which applies when equilibrium between material temperature and thermal radiation temperature is reached.

Numerical results are calculated for various yields and yield pulse shapes. These results are compared to those predicted by the model previously developed by G. C. Pomraning.

The model developed here predicts reasonable numerical results and physically reasonable time dependences. It does not entail integrations over retarded time or the use of moments of radiation transport equations. It engenders an intuitive understanding of the fireball growth process and was developed for pedagogical use.

I. Introduction

A. Background

1. Fireball Radiative Growth Phase. This thesis deals with the radiative growth phase of the development of the x-ray fireball from an atmospheric nuclear explosion. During this phase, x-rays from the device heat the surrounding air to a high level of ionization. A thermal radiation field builds up as a result of re-emission of photons by the air. The fireball grows as photons from the device stream outward to be absorbed in the ambient air surrounding the fireball. The other mechanism of transport of energy outward is the diffusion of the thermal radiation in the fireball. During this phase, energy transport to the surface of the fireball is accomplished only by radiative transport because the growth is at a rate faster than a material shock wave can propagate through the fireball, even under the extreme pressures and temperatures. This radiative phase ends at hydrodynamic separation, when the radiative transfer has decreased enough that the shock front can travel as fast as the fireball radius.

2. Modeling the Radiative Growth. The standard reference in the field, "The Effects of Nuclear Weapons" [Ref 1] provides qualitative information about the radiative

growth of a nuclear fireball, but no mathematical model of the processes. G. C. Pomraning has published such a mathematical model [Ref 2], referred to here as the "early time model", following the title of his paper. Reference 3 develops the model in more detail, including presentation of a finite differencing scheme for implementing the model. His model allows the computation of the material temperature and thermal radiation temperature but is limited in its effectiveness for pedagogical use by its complexity, as well as for other reasons examined in detail later.

3. Pedagogical Model. There exists the need for a mathematically simple model which is based on the physical processes of the radiative fireball growth. This model is needed for pedagogical use in programs such as the Nuclear Weapons Effects curriculum at the Air Force Institute of Technology, where this research was done. Such a model should predict numerically and physically reasonable results and should engender an intuitive physical understanding of the nuclear fireball radiative growth.

B. Problem and Scope

The objective of this research has been to develop a physically meaningful model of the growth of a fireball from an atmospheric nuclear detonation up to the point of hydrodynamic separation which:

-- is appropriate for instruction at the graduate level without requiring a previous knowledge of transport theory or advanced mathematical or numerical methods

-- is based on simple models of the physical processes

-- predicts temperatures and time dependences of the right order of magnitude

-- predicts curves of radius and temperatures with physically reasonable shapes.

The second objective of this research has been to verify these characteristics by:

-- implementing the model in a computer program

-- graphing the results for various combinations of yield, pulse duration, and pulse shape

-- comparing to results obtained using the early time model as a benchmark.

The scope of the project has been limited to the consideration of the radiative transport phase only. The examples computed for evaluation and comparison include two nuclear pulse shapes, a square wave and an isosceles triangle. The examples all assume sea level ambient air density.

C. Assumptions

All the models presented here assume that the nuclear

detonation is a free air burst in uniform air, that the nuclear device is a point source of energy in the atmosphere, and that the fireball is homogeneous.

D. Approach and Presentation

The sequence of presentation of this thesis follows the approach used in the research. Section II summarizes the early time model and presents the results of its application to an example problem. Difficulties with the model are considered. Section III considers the approach to be used in developing a new model. Similarities with the early time model, and assumptions in common are presented, followed by differences and additional assumptions. Section IV develops the homogeneous three-temperature model using energy balance equations. This model applies when the temperatures are not yet in equilibrium. A finite differencing algorithm is presented. Section V develops the homogeneous one-temperature model which applies after equilibrium has been established between the material temperature and the thermal radiation temperature. Section VI presents the results of numerical calculations using the combined homogeneous model, and comparing the results to those obtained using the early time model. Section VII evaluates the pedagogical and numerical advantages and limitations of the homogeneous model, and conclusions and recommendations are presented in section VIII.

II. Background: Pomraning's Early Time Model

A. Characteristics of the Radiative Growth Phase

The radiative growth phase of fireball formation could be divided into subphases based on several possible distinctions. Among these are (1) burnout vs. not fully ionized; (2) energy transport mechanism; (3) equilibrium vs. nonequilibrium of material temperature and thermal radiation temperature. The assumptions chosen in regard to these characteristics largely determine the nature of the model derived. Therefore, these distinctions will be described before the assumptions for the early time model and for the homogeneous models are presented.

1. Burnout. At the beginning of fireball formation, the volume of the fireball is small. Therefore, the radiation is so intense as to fully ionize, i.e. burnout, the air in the fireball. Any time an electron reattaches to a nucleus (emitting a photon of thermal radiation), it immediately absorbs another photon of streaming radiation and the atom is again fully ionized. Thus, the material temperature, T_m, is maintained at the burnout temperature, T_b, approximately 400 eV [Ref 2]. As the fireball becomes larger, and (eventually) as the production of streaming radiation by the nuclear explosive decreases, the radiation becomes less intense. At some point, atoms which form are no

longer immediately re-ionized, and the fireball cools. At this point, the burnout subphase is completed.

2. Energy Transport Mechanism. There are two energy transport mechanisms available during the radiative growth phase. These are: streaming of radiation from the nuclear explosive directly outward through the fireball, and diffusion of the thermal radiation produced in the volume of the fireball. At the beginning of fireball formation, the streaming radiation is intense and the thermal radiation is negligible, so the mechanism is streaming only. Eventually, the yield pulse is over and the streaming radiation has been absorbed, but the thermal radiation has built up significantly, so the mechanism is diffusion only. The transition from streaming only to diffusion only is a smooth one, so for some intermediate interval the transport mechanism is both streaming and diffusion.

3. Equilibrium. At the beginning of fireball formation, the material is heated (essentially instantly) to burnout temperature but the thermal radiation field takes time to build up. Conditions start far from equilibrium: $T_m = T_b$ but $T_{eff} = 0$, where T_{eff} is the effective (black body equivalent) temperature of the thermal radiation. While the streaming radiation is intense, and the fireball is rapidly growing (diluting the thermal radiation as it builds up), this nonequilibrium condition will be maintained. Eventually, however, equilibrium will be closely approached.

B. Major Assumptions of the Early Time Model

The early time model divides the radiative growth phase into two distinct subphases, burnout and diffusion. During the burnout subphase, the mechanism of energy transport is assumed to be streaming only. During the post-burnout period, the mechanism is assumed to be diffusion only.

The early time model assumes that streaming radiation is absorbed at whatever rate is required to maintain T_m at T_b. This is equivalent to assuming that the air is opaque to streaming radiation ($K_s = \infty$) if $T_m < T_b$ and transparent to streaming radiation ($K_s = 0$) if $T_m > T_b$. Thus, the model assumes that the breakpoint between burnout and cooling and the breakpoint between streaming only and diffusion only occur simultaneously. The model further assumes that there is no overlap period of transport by simultaneous streaming and diffusion.

The model assumes nonequilibrium of temperatures throughout both subphases. The model predicts, numerically, the close approach to equilibrium, but does not require equilibrium as a simplifying assumption.

The early time model assumes that the burnout phase ends when one of the following conditions is met (whichever occurs first):

— The streaming radiation intensity at the surface of the fireball falls to zero, or

— All of the yield delivered so far is accounted for as material and thermal radiation energy of the fireball.

The early time model uses very different techniques for modeling the two phases, burnout and diffusion. These two approaches are discussed next.

C. Burnout Phase Approach

Consider the fireball at a time t, at which it has a radius R, with streaming radiation energy density $E_s(r,t)$. Then energy which streams through the boundary at R in a time increment dt is $4\pi R^2 c E_s(R,t) dt$. This energy burns out an additional shell of thickness dR containing material and streaming energy of $4\pi R^2 dR (E_s(R,t) + E_b)$, where E_b is the energy density of the air at burnout. An energy balance of these two expressions can be solved for dR/dt, if $E_s(R,t)$ is known.

The source of $E_s(R,t)$ is yield which was delivered at a retarded time $t' \equiv t - R/c$ and which is subject to absorption as it travels from $r = 0$ (at t') to $r = R$ (at t). Therefore, an integral over this path is required to find the absorption loss. This path integral can be treated equivalently as an integral over retarded time from t' to t. As the streaming radiation passes a radius r" at time t" (dummy integration variables), the absorption is found by the requirement that it be exactly enough to maintain the material temperature at burnout, i.e. $T_m = T_b$ so the energy

absorbed from streaming radiation equals that added to thermal radiation. The net production rate of thermal radiation depends on the emission rate, which is constant since $T_m = T_b$, and the absorption rate, which is proportional to the thermal radiation energy density, E_t. So, knowledge of $E_t(t)$ is required for the integration which gives $E_s(R,t)$, which is required to obtain dR/dt.

Since E_t is produced at a constant rate by emission from the air at T_b, it would build up exponentially to equilibrium, except that it is also subject to dilution as R increases. So knowledge of $E_t(t)$ requires knowledge of R(t).

The result of the approach is a model consisting of a coupled system of integral and differential equations which must be solved numerically. Further details of these equations will not be provided here, since this summary is intended only to provide a conceptual overview of Pomraning's work. Details can be found in either reference 2 or reference 3.

D. Diffusion Phase Approach

For the diffusion phase, Pomraning first assumes that the diffusion equation is valid, and that the material and thermal energy densities are not necessarily spatially uniform. He further assumes that $E_t = \epsilon a T_m^4$ where ϵ varies with time, but is spatially uniform at each time. This is combined with an assumed cubic temperature

dependence of the mean free path of thermal photons to simplify the diffusion equation. The first and second moments of the diffusion equation are then taken. These moment equations are then simplified by applying the assumption that all the energy densities E_t, E_s and E_m are spatially uniform inside and zero outside the fireball.

These assumptions result in a coupled system of differential equations which must be solved numerically. Again, the details are left to reference 2. The results of calculations using the early time model for an example case are presented next, followed by an evaluation of some difficulties observed.

E. Example Case Using the Early Time Model

As an example of the application of the early time model, a 20 kiloton burst, with a constant yield delivery rate of 3.8873 kilotons/shake and with 5.14493 shakes duration, was analyzed. This pulse duration was chosen to provide the same yield delivery rate as the peak value for the double-exponential pulse considered in reference 2.

Figures 1 through 3 show the material and radiation temperatures, the radius, and the growth rate, dR/dt, over the first 20 shakes, starting at the beginning of the burst. Observations about these curves are presented in section F, below. Examples of other yields, pulse shapes, and pulse durations are provided in Appendix A.

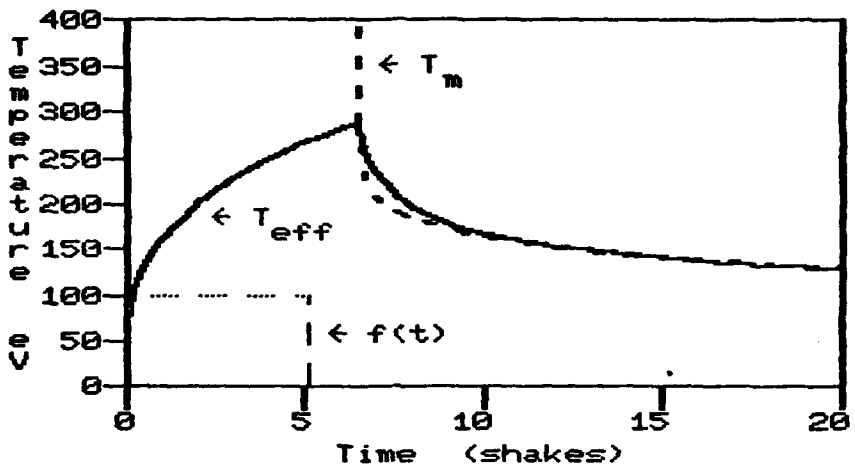

Fig. 1 Material and Effective Radiation Temperature

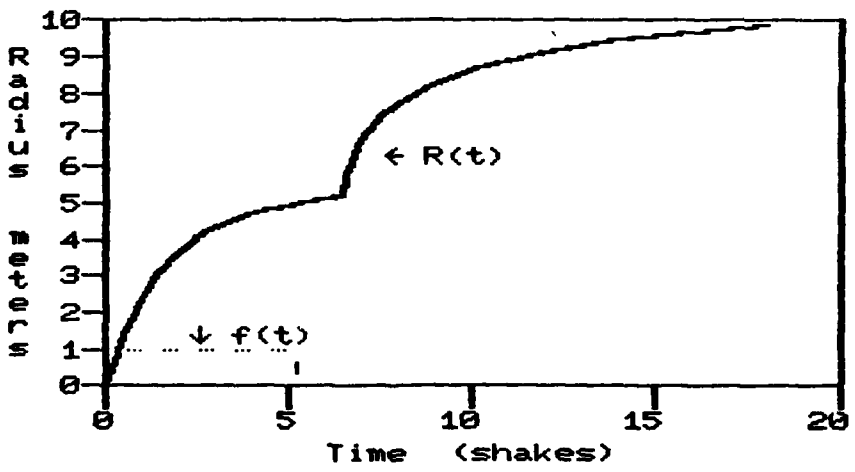

Fig. 2 Radius, Early Time Model, 20KT

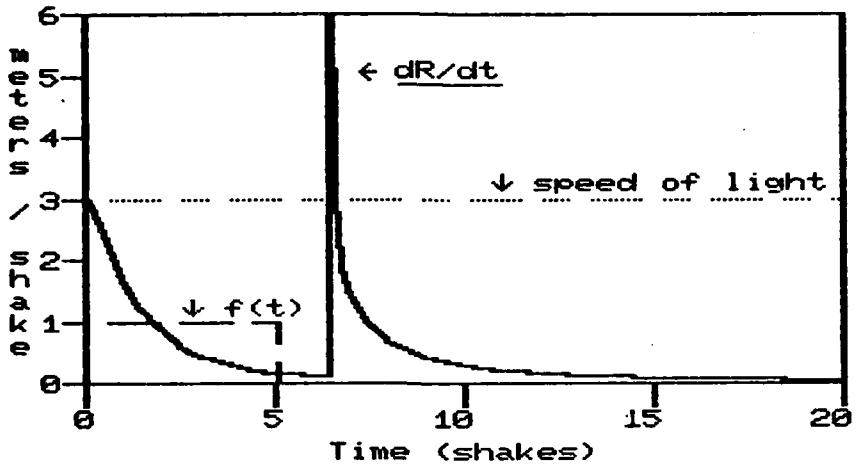

Fig. 3 Growth Rate, Early Time Model, 20KT

F. Predictive Problems of the Early Time Model

The example curves presented above illustrate some problems with the results predicted by the early time model.

1. Effective Temperature. T_{eff} should be a smoothly varying function of time, yet figure 1 shows a sudden break in slope at the transition between burnout and diffusion phases.

2. Decreasing Fireball Expansion Rate. dR/dt should be a monotone decreasing function of time unless the yield rate is rapidly increasing, which is never the case for the example square wave pulse. In particular, when the streaming radiation is fully absorbed, dR/dt should decrease because of the less efficient transport of energy by diffusion alone, rather than diffusion and streaming together. However, figure 3 shows a step increase in dR/dt at the end

of the burnout phase.

3. Constraint by the Speed of Light. The expansion rate of the fireball should never exceed c, the speed of light (3 meters/shake). However, the early time model predicts an interval at the beginning of the diffusion phase in which dR/dt is greater than the speed of light.

4. T_m versus T_{eff}. The material temperature, T_m, should always exceed the thermal radiation effective temperature, T_{eff}, since emission by the material is the only source of thermal radiation and since the radiation is continually leaking out of the fireball interior whereas the material energy cannot leak. However, figure 1 shows a rapid drop in T_m at the beginning of the diffusion phase, until T_m is less than T_{eff}. T_{eff} then approaches equilibrium with T_m from above, rather than from below.

6. Causes of the Predictive Problems

1. Effective Temperature. The sharp peak in T_{eff} at the end of the burnout phase is caused by not accounting for diffusion transport as E_t becomes significant and E_s becomes small. This has two related effects: E_t is not lost (in the model) by conversion to E_m as it diffuses into ambient air and is absorbed, and dR/dt is underestimated, so the tendency to decrease E_t by dilution is underestimated. Both effects cause E_t to rise too steeply and too high during the latter part of the burnout phase.

2. Decreasing Fireball Expansion Rate. The step increase in dR/dt at the end of the burnout phase arises from this same cause. dR/dt is underestimated at the latter part of the burnout phase because the diffusion transport is ignored. The effect is exacerbated by the overestimation of T_{eff} and E_t, since this leads to an overestimate of dR/dt in the beginning of the diffusion phase.

3. Constraint by the Speed of Light. The early time model predicts a rate of expansion of the fireball which exceeds the speed of light during the diffusion phase because dR/dt is not being modeled directly. The moments equation method does not reflect the physical constraint of $dR/dt < c$.

4. T_m versus T_{eff}. The early time model predicts $T_m < T_{eff}$ during the diffusion phase because the moments equations do not directly model the process of conversion of E_t to E_m as the fireball expands.

H. Pedagogical Difficulties

1. Integrals over Retarded Time. The retarded time and path integrals can be confusing. The physics is obscured by the mathematics. For the beginning graduate student with a general engineering background, without specific preparation in transport theory or in the use of retarded potentials in electromagnetics, this can be a problem.

2. Moments of a Diffusion Equation. Although the diffusion equation is familiar to the student, in terms of neutron diffusion and Fick's Law, the use of moments equations may be accepted (intellectually) as a legitimate mathematical manipulation but without leading to an intuitive physical understanding. The moments equations are particularly hard to accept when applied to a homogeneous fireball with a step decrease to zero energy densities at its surface, since the diffusion equation is not valid near the discontinuity and predicts no net energy transfer elsewhere. A more involved derivation of the same final equations directly from the full Boltzmann equation might be possible, but this would present its own problems, since the student would not have the necessary background in transport theory, in most cases.

3. Computational Difficulty. The early time model does not lend itself well to use as a calculational exercise or project. A straightforward finite differencing scheme can be presented, but the integrals over retarded time require maintaining several vectors of past variable values amounting to an array of several thousand floating point numbers. This precludes the use of personal microcomputers and results in more loading of main frame facilities. Calculation of the numerical integrations at each time step also results in relatively long (expensive) execution times.

The computations for the examples in this thesis were actually performed on a personal microcomputer, but this required the derivation of a system of recursive equations which could be iterated at each time step to obtain the needed retarded time integrals, together with the use of programming tricks to increase speed at the expense of intelligibility of the program source code. The recursion system is presented in Appendix D. This would not make the model useful as a programming project, however, because as much time could be spent presenting the programming techniques as would be spent presenting the physics.

4. Predictive Problems. The prediction, numerically, of physically unreasonable behaviors, as discussed above, presents problems in the pedagogical use of the model. The student would (one hopes) be unsatisfied with an understanding which is founded on a model which predicts unreasonable behaviors through limitations which are not understood. The difficulty is that to see the causes of the predictive problems of the early time model requires at least as good an understanding of the physics as the model is intended to create.

I. Conclusions

A successful pedagogical model should avoid the use of retarded time and of moments equations. A finite differencing scheme should follow from the model in a direct

way. The differencing scheme should be programmable as an exercise using limited computer resources, such as personal microcomputers. The numerical predictions of such a program should be physically reasonable. The model should be based on simple mathematical models of the relevant physical processes. The next section will present an approach, together with its major assumptions, which is then used to develop a model to meet these goals. These assumptions are selected so as to avoid those major assumptions which led to difficulties with the early time model.

III. Approach and Assumptions

A. Approach

The approach used in choosing assumptions for the model to be developed in subsequent sections is to retain as much as possible of the early time model. Those assumptions which lead to physically unreasonable numerical results or to pedagogical difficulties were identified in the previous section. Those assumptions are replaced by alternative choices as described below.

B. Assumptions Retained from the Early Time Model

1. Infinite, Homogeneous Ambient Air. The energy release from the nuclear explosive device is assumed to occur in an infinite volume of air of uniform thermodynamic properties. This is a reasonable assumption because the diameter of the fireball at hydrodynamic separation is on the order of tens of meters (about 25 meters for 20 kilotons) [Ref 1.65] while the atmospheric density varies approximately exponentially with a scale height of roughly 7 km (at sea level) [Ref 4]. This also assumes that the burst is higher off the ground than the radius of the fireball at hydrodynamic separation. The presence of the ground could be incorporated into the model, as will be

explained in the development of the model, but the ground is not explicitly considered here because it is does not add significant physics to the model.

2. Point Source Nuclear Device. The explosive is assumed to be a point source of energy release in the atmosphere. This assumption can be viewed in either of two ways. First, the assumption is equivalent to assuming that the structure which surrounds the actual nuclear fuel behaves the same as the air. Alternatively, any effects of this structure can be considered to have been incorporated in the choice of the total (x-ray) yield and the normalized yield release rate function, f(t).

3. Homogeneous Fireball. The conditions inside the fireball, in particular the energy densities E_m and E_t, are assumed to be spatially uniform throughout the radiative phase of the fireball growth. At burnout, the mean free path of photons is about 50 meters, which is large compared to the fireball radius, so the assumption is initially an excellent one. By the time of hydrodynamic separation, at about 25 eV [Ref 1.65], the mean free path is about 1/3 meter, so the homogeneous assumption constitutes a limitation of the model by the end of the radiative growth phase.

4. Yield Rate Function: f(t). The normalized yield delivery rate function, f(t), may be any specified (non-negative) function of time. The examples used here

assume square pulses or triangular pulses for convenience, but the model can utilize whatever time dependence is desired, such as the double-exponential pulse used by Pomraning in reference 2.

5. Numerical Values of Parameters. The values of parameters, such as air density and opacity, are taken from reference 2. This assures comparability of the results of the two models.

6. No Motion of Material Inside the Fireball. Heat transfer by conduction, convection, or bulk motion is neglected. This is reasonable because of the short time scale and because the fireball expands faster than the speed of sound in the fireball during the radiative phase, by definition.

C. Assumptions Revised from the Early Time Model

As described in section II.A, the major assumptions of a model concern burnout, energy transport mechanisms, and equilibrium. The major assumptions needed for the homogeneous models developed here are presented in that order.

1. Burnout. Difficulties with the early time model arose from the assumption that burnout is maintained until the streaming radiation has been fully absorbed. For the homogeneous models, it is instead assumed that burnout is maintained only until the absorption rate required to maintain burnout exceeds the ability of the air, at burnout

opacity, to absorb energy from the field of streaming radiation present. The details of mathematically modeling this condition for the end of the burnout subphase are developed in section IV.E.3. The assumptions about opacity of the air needed for that development are discussed next.

2. Opacity of the Air to the Thermal Radiation.

The air opacity to thermal radiation, K_t, is assumed to be an inverse cubic function of the energy of the thermal photons: $K_t \sim (1/h\nu)^3$. Since the energy of the thermal photons is proportional to the material temperature of the air that emitted them, it is equivalently assumed that the opacity is an inverse cubic function of the air temperature, for temperatures up to burnout temperature. However, since the main interactions are bound-free, the air is assumed to be transparent when fully ionized, so that K_t is assumed to be zero above T_b. Thus, dropping the subscript "t" for reasons discussed in paragraph 3, below:

$$\begin{aligned} &\text{For } T_m < T_b \\ &\qquad K(T_m) = K_b \left[T_b/T_m\right]^3 \\ &\text{For } T_m > T_b \\ &\qquad K(T_m) = 0 \end{aligned} \tag{1}$$

where K_b means $K(T_b)$.

3. Opacity of the Air to Streaming Radiation.

As for the thermal radiation, the opacity to streaming radiation is an inverse cubic function of the streaming radiation photon energy, hence of the streaming radiation source temperature, T_s. However, T_s is a complex function of time and is dependent upon the design and construction of the nuclear explosive, and is not presumed to be known. It is known that $T_s > T_m$ (otherwise the heat transfer would be inward). Therefore, the opacity to streaming radiation is less than the opacity to thermal radiation. The three-temperature model uses this bounding value, κ_t, as the value for κ_s, which must be recognized as an approximation. This is a better approximation than the early time model's assumption of infinite opacity to streaming radiation. Both opacities, κ_t and κ_s, will subsequently be referred to as κ without subscript and without distinction between them.

4. Energy Transport Mechanisms. Predictive difficulties with the early time model arose from the assumption that a period of streaming only transport is followed by a period of diffusion only transport, with no period of overlap. Pedagogical difficulties arose from the techniques used to model these two transport mechanisms, namely the integrations over retarded time, and the moments equations. To avoid these difficulties, three major assumptions are made.

a. Streaming Mechanism. It is assumed that the rate of transfer of energy by streaming through the total surface area of the fireball is given by

$$\{\text{Streaming Rate through Surface}\} = c\,E_s\,A \qquad (2)$$

where, by definition,

$$A = \{\text{area of the fireball surface}\} \qquad (3)$$

$$E_s = \{\text{average value of the streaming radiation density in the fireball}\} \qquad (4)$$

This is the same model used in the the burnout phase of the early time model except for the additional assumption that E_s is uniformly distributed throughout the fireball, so the value of E_s at the surface is just the average value of E_s inside the fireball. This assumption eliminates the need for integrals over retarded time.

b. Diffusion Mechanism. It is assumed that the corresponding energy transfer rate for diffusion of the thermal radiation is given by:

$$\{\text{Streaming Rate through Surface}\} = \frac{c}{4}\,E_t\,A \qquad (5)$$

This assumes that radiation streams at speed c but diffuses at speed c/4 and is equivalent to assuming the radiated power equals that of a black body in equilibrium at a temperature of T_{eff} as is shown in section IV.F.1.b.

c. Overlap Period. It is assumed that streaming transport occurs as long as there is streaming radiation present in non-negligible amounts. It is assumed that diffusion cannot transport energy through the fireball surface to contribute to the growth rate as long as the fireball is expanding at a rate greater than c/4 due to the streaming radiation. Conceptually, this is because the thermal radiation can't diffuse outward fast enough to keep up with the surface, which is ever receding away from it. Thus, there is an overlap period of transport by streaming and diffusion both. This overlap period starts when dR/dt falls to c/4 and lasts until the streaming radiation becomes negligible (in the equilibrium model, discussed below). Because of this overlap period, the three-temperature homogeneous model has smooth transitions and behaves as a single, continuous model, unlike the early time model with its two distinct phases.

5. Equilibrium. While the early time model never explicitly assumes equilibrium, it will be necessary to do so for the one-temperature homogeneous model. The approach used is to develop the three-temperature homogeneous model from the assumptions presented above. The model predicts, numerically, that equilibrium is closely approached some tens of shakes after the streaming radiation becomes negligible. However, the three-temperature finite differencing scheme becomes unstable when equilibrium is

approached too closely. (This instability is discussed in the final paragraph of Appendix B.) Therefore, it is necessary to assume equilibrium at this point, and a one-temperature model is used for the remainder of the computations. (In practice, the cross-over point between the two numerical methods was established manually by examination of the output of the finite differencing scheme.) The one-temperature model incorporates all the same assumptions and modeling of the physical processes that are developed for the three-temperature model, so the difference is only of computational, rather than conceptual, significance. Therefore, the combination of the two will be referred to as the homogeneous model.

IV. Noneguilibrium Phase:
Three-Temperature Homogeneous Model

A. The Three Energy Densities

The energy of the fireball is partitioned among three distinct forms: streaming radiation, material heat, and thermal radiation. The three temperatures are T_s, T_m and T_{eff} and are defined next.

1. Streaming Radiation. The streaming radiation comes directly from the nuclear explosive device with an energy distribution which may or may not be Plankian. Since this analysis uses the (bounding) value of the fireball opacity to thermal radiation as an approximation for the opacity to streaming radiation (see section III.C.3), the source temperature of the streaming radiation, T_s, is not of concern. Therefore, the streaming radiation will be characterized only by its energy density, E_s.

2. Material Energy. The material energy is characterized by its thermodynamic temperature, T_m. The ions and electrons of the fireball plasma are assumed to be in thermodynamic equilibrium (with each other), so distinct ion and electron temperatures are not considered. Since the heat capacity is assumed constant, the energy density of the material is:

$$E_m = c_v T_m \tag{6}$$

3. Thermal Radiation. The thermal radiation will not be in black body equilibrium during this phase, but is approaching such equilibrium. Therefore, it is reasonable to characterize the thermal radiation field by the temperature of a Plankian distribution of equal energy density. This "effective temperature" is defined by the relation:

$$E_t = aT_{eff}^4 \tag{7}$$

B. Physical Processes

The physical processes considered in the model are summarized here and detailed in the rest of this section.

1. Streaming Radiation Processes. The streaming radiation is emitted from the nuclear explosive device. It enters the fireball at its interior boundary. It is subject to absorption within the fireball as it streams radially to the exterior boundary. At the surface of the fireball, the streaming radiation enters the (cold) ambient air, and is absorbed in a short distance, on the order of a mean free path of an x-ray in ambient air (a few cm). Thus, one may visualize a thin absorption layer on the surface of the fireball. The ambient air in this layer is heated to the fireball material temperature, T_m, ionizing it and advancing the surface of the fireball outward. In a time increment dt, the radius of the fireball is increased by dR, producing an additional volume, dV, of air heated to T_m and filled with streaming energy at density E_s. The shell of thickness dR

which constitutes dV is not the thin absorption layer, but rather is the volume swept out by the advancing surface of the fireball in the time increment dt. Since the major assumption of this model is that temperatures are homogeneous inside the fireball and zero outside the fireball, this requires the idealization that the absorption layer is of zero thickness. In recognition of this, this absorption of radiation will be referred to as absorption at the surface of the fireball.

2. Material Energy Interactions. Because the period modeled here is entirely before hydrodynamic separation, heat conduction, convection, or other direct interaction are neglected; radiative interactions only are considered. These interactions occur both within and at the advancing surface of the fireball. Within the fireball, material energy is produced by absorption of streaming and thermal radiations; material energy is lost by emission of thermal radiation. These interior effects tend to raise or lower the temperature, T_m. As the surface advances, material energy is produced by absorption of streaming and thermal radiations, causing fireball growth rather than temperature changes.

3. Thermal Radiation Processes. The thermal radiation is formed by emission throughout the volume of the fireball. It is also absorbed within that region. Thermal radiation moves to the surface of the fireball by diffusion and is absorbed there.

C. Total Energy Balance Equations

1. General Global Balance Equation. The differential equations of the three-temperature model will be developed by means of global energy balances on each of the three energies. By global balance, I mean the energy density integrated over all space (the total energy, Q) balanced before and after a time increment, dt. Such balances are simplified by the assumption that the energy densities are spatially uniform inside the fireball and zero outside the fireball. Thus:

$$Q_x \equiv \text{(Total Energy of form x at time t)} = \int E_x(r,t)\, dV = V_{fireball}\, E_x(t) \qquad (8)$$

where 'x' indicates streaming or material or thermal.
The global energy balance equations are of the form

"New Value = Old Value + Production in dt - Loss in dt"

It is useful to distinguish between production/loss occurring in the fireball interior and production/loss occurring at the surface because of the different nature of these processes. With this distinction, the general global balance equation becomes:

(Total energy Q_x at time t+dt) = (9)

(Total energy Q_x at time t)

\+ (Energy Q_x produced inside during dt)

\- (Energy Q_x absorbed inside during dt)

\+ (Energy Q_x produced at surface during dt)

\- (Energy Q_x absorbed at surface during dt)

where 'x' indicates streaming or material or thermal.

2. Production and Loss at Surface of Fireball. By definition, during time interval dt, the fireball grows in volume by the addition of a shell of thickness dR and volume dV onto the original fireball of radius R and volume V, producing a new radius R' and volume V' at time t' = t+dt. The conversion of energy at the surface during dt can most easily be visualized using these terms, and is described next.

For streaming and thermal radiation energies, there is no production at the surface. Absorption occurs on the surface, which moves from R to R' during dt. This absorption is found by:

(Radiation energy Q_r absorbed at surface during dt) =

(Radiation energy Q_r which enters dV

through surface at R during dt) (10)

− (Radiation energy Q_r which is still present

in dV as radiation energy of type r at time t')

where 'r' indicates streaming or thermal.

For material energy, there is no loss on the surface. The production on the surface (by absorption of streaming and thermal radiation) is found by:

(Material energy Q_m produced at surface during dt) =

(Material energy Q_m present in dV at time t') (11)

3. Production and Loss Inside the Fireball. The average volume of the fireball during dt is:

$$V_{ave} = V + dV/2 \tag{12}$$

and the interior conversion of energy can be visualized as:

$$\left(\begin{matrix}\text{Absorption}\\ \text{Production}\end{matrix}\right. \text{ of energy Qx inside fireball during dt) =}$$

$$\left(\begin{matrix}\text{Absorption}\\ \text{Production}\end{matrix}\right. \text{ rate of energy density Ex at t) * } V_{ave} \text{ * dt} \tag{13}$$

where 'x' indicates streaming or material or thermal, and the absorption/production rate is assumed constant during dt.

Next, the various production and loss mechanisms will be considered and rate equations developed. The results will then be substituted in the global energy balances to obtain the desired differential equations and finite difference equations.

D. Center Point Boundary Conditions

The energy release is assumed to be from a device of negligible volume (a "point source"). Therefore, the interior boundary reduces to a center point for the purpose of specifying boundary conditions. These boundary conditions are simplified by the assumptions that each energy density is spatially uniform within the fireball (3-temperature-homogeneous) and that the material and the thermal radiation do not interact directly with the explosive device. Consequently, E_m and E_t automatically meet the requirements of finiteness, continuity, and no net flux through the interior boundary. Thus, no interior boundary conditions need be explicitly specified for E_m and E_t.

The streaming radiation enters the fireball from the point source. The associated boundary condition can be treated as a term in the global balance equation for the streaming radiation energy as follows:

(Streaming energy produced inside (at center of) fireball during dt) = $Y f(t) dt$ (14)

where Y is the Yield.

E. Equilibration Relations Within the Fireball

1. Emission of Thermal Radiation. The thermal radiation is emitted at a rate proportional to the density of air, ρ, its opacity, κ, (which, as described in section III.C, is assumed to be an inverse cubic function of its temperature) and to the temperature to the fourth power as follows:

$$\frac{d}{dt} E_{t\ emission} = C(T_m)\ aT_m^4 \qquad (15)$$

where

$$C(T_m) = \rho c \kappa_b\ (T_b/T_m)^3 \qquad (16)$$

so that

(Thermal radiation energy produced in fireball during dt)

$$= C(T_m)\ aT_m^4\ V_{ave}\ dt \qquad (17)$$

= (Material energy lost inside fireball during dt)

2. Absorption of Thermal Radiation. The thermal radiation is absorbed at a rate proportional to the density of thermal radiation present to be absorbed, and with the same proportionality coefficient as for emission. Thus:

$$\frac{d}{dt} E_{t\ absorption} = -\ C(T_m)\ E_t \qquad (18)$$

and

(Thermal radiation energy absorbed inside fireball during dt)

$$= C(T_m)\ E_t\ V_{ave}\ dt \qquad (19)$$

3. Absorption of Streaming Radiation. A portion of the streaming radiation is absorbed by the ionized air in the fireball. The rate of absorption depends on the conditions in the fireball in the following way:

If $T_m = T_b$ and $[aT_m^4 - E_t] < E_s$ then

(Streaming energy absorbed inside fireball during dt)

$$= C(T_m)\,[aT_m^4 - E_t]\,V_{ave}\,dt$$

otherwise

(Streaming energy absorbed inside fireball during dt)

$$= C(T_m)\,E_s\,V_{ave}\,dt \qquad (20)$$

In general terms, there are two criteria to consider: the streaming radiation can be intense or weak; the fireball can be at burnout or below burnout. If the fireball is below burnout and the streaming radiation is weak, then the absorption of streaming radiation will be less than the net loss of E_m by emission of thermal radiation. The fireball will be cooling.

Conversely, if the fireball is below burnout and the streaming radiation is intense, then the absorption of streaming radiation will exceed the net loss of E_m by emission of thermal radiation. T_m will be rising.

But if the fireball is already at burnout, then it cannot absorb more streaming radiation than it loses to thermal radiation, because that would raise its temperature

above burnout, which would make it transparent, preventing absorption of streaming radiation. So no matter how intense the streaming radiation, the fireball can only absorb enough to maintain T_b, i.e., enough to equal the net loss of E_m by emission of thermal radiation.

The final case to consider is if the fireball is at burnout and the streaming radiation is weak. In this case, the absorption of streaming radiation is small and the fireball cools, as in the first case.

In order to quantify these arguments, consider first the cases where $T_m < T_b$. Since the same value of opacity is being assumed for the streaming radiation as for the thermal radiation, the absorption rate of streaming radiation density, E_s, depends upon the air density, the opacity, and upon E_s in the same way as shown above in the case of absorption of thermal radiation. Thus, the rate of absorption of streaming radiation is given by:

$$\left(\begin{array}{l}\text{Total Streaming Energy, } Q_s, \\ \text{absorbed inside fireball during dt}\end{array}\right) = C(T_m)\, E_s\, V_{ave}\, dt \qquad (21)$$

In the case where $T_m = T_b$ and the streaming radiation is weak, this same relation holds. If the streaming radiation is intense, however, the absorption of streaming radiation cannot be large enough to cause the air temperature to rise, as described above. Thus, the rate of absorption of

streaming radiation cannot exceed the amount needed to maintain the air temperature at burnout, which is equal to the net loss rate of material energy (by emission and absorption of thermal radiation). Hence, the absorption rate of streaming radiation is bounded by:

$$\left\{\begin{array}{l}\text{Net loss of } Q_m \text{ by emission of} \\ Q_t \text{ inside fireball during } dt\end{array}\right\} = C(T_m)\,[aT_m^4 - E_t]\,V_{ave}\,dt \qquad (22)$$

Thus, if $T_m = T_b$ then the absorption is given by equation (21) unless it would exceed the bound given by equation (22), i.e. unless $[aT_m^4 - E_t] < E_s$.

Combining equations (21) and (22), together with their conditions of applicability, gives the result initially stated, equation (20).

4. Production of Material Energy. Material energy is produced inside the fireball by absorption of both streaming and thermal radiation. Combining equations (19) and (20) gives the term needed for the global balance equation for material energy:

If $T_m = T_b$ and $[aT_m^4 - E_t] < E_s$ then

{Material energy produced inside fireball during dt}

= {Material energy absorbed inside fireball during dt}

otherwise

{Material energy produced inside fireball during dt}

$$= C(T_m)\,[E_s + E_t]\,V_{ave}\,dt \qquad (23)$$

F. Fireball Growth: Surface Boundary Conditions

1. Energy Transport. Energy is transported to the surface of the fireball by two mechanisms of radiative transport, streaming and diffusion.

a. Streaming. Transport of the streaming radiation causes energy to arrive at the surface, radius R, at a rate of cE_s per unit area, since E_s is assumed uniform throughout the fireball. Thus, in terms of a global energy balance, the total rate of energy arriving at the surface of the fireball is cE_sA where A is the area of the surface, and

(Streaming radiation energy which enters dV through surface at R in time dt) $= c E_s A \, dt$ (24)

b. Diffusion. Transport of the thermal radiation is by diffusion. This process is essentially that of a radiating black body at a temperature of T_{eff}, which would radiate with power per unit area of σT_{eff}^4 Since $\sigma = \frac{c}{4} a$ the total rate of arrival of thermal radiation at the (stationary) surface is

$$\sigma T_{eff}^4 A = \frac{c}{4} E_t A \quad (25)$$

(Thermal radiation energy which enters dV through surface at R in time dt) $= \frac{c}{4} E_t A \, dt$ (26)

2. Fireball Growth. The growth of the fireball is determined by an energy balance on the incremental volume, dV, burned out in time increment dt. There are three possible cases to consider. These consist of growth caused by streaming only, by diffusion only, and by both together.

a. Growth by Streaming Only. In this case, the energy balance requires that the energy entering dV, by streaming through the surface, must equal the energy density in dV times dV. Thus, since only streaming radiation enters dV:

$$c\, E_s\, A\, dt = (E_s + E_m)\, dV \qquad (27)$$

Solving:

$$\frac{dV}{dt} = A\, c\, E_s / (E_s + E_m) \qquad (28)$$

This case applies when the streaming radiation is so intense as to cause dR/dt > c/4 so that the diffusion of thermal radiation essentially cannot keep up with the advancing surface of the fireball. This is an approximation since some thermal photons must be directed nearly directly outward, but this approximation will prove to be a useful one.

b. Growth by Diffusion Only. In this case, the energy balance is the same as for streaming, but E_s is replaced by E_t and c by c/4, since radiation streams at c but diffuses at c/4. Thus:

$$\frac{c}{4}\, E_t\, A\, dt = (E_t + E_m)\, dV \qquad (29)$$

Solving:

$$\frac{dV}{dt} = A \frac{c}{4} E_t / (E_t + E_m) \qquad (30)$$

This case applies when the streaming radiation density becomes negligible, which is somewhat later than the end of the yield pulse which produces the streaming radiation.

c. Growth by Diffusion and Streaming Superposed. In this case, the energy balance on dV assumes that dV is filled with streaming and thermal radiations at the same densities as in the interior of the fireball. The excess of energy entering dV is present as material energy at the same temperature as inside the fireball. Thus:

$$A (c E_s + \frac{c}{4} E_t) dt = (E_s + E_t + E_m) dV \qquad (31)$$

Solving:

$$\frac{dV}{dt} = A c (E_s + E_t/4) / (E_s + E_t + E_m) \qquad (32)$$

This case applies when $dR/dt < c/4$ and both streaming and thermal radiations are present. Note that if $dR/dt = c/4$, then both equation (28) and equation (32) give the same result, even if $E_t > 0$. Thus, the change from streaming only to both streaming and diffusion is a smooth one. Note also that equations (29) and (30) are special cases of equations (31) and (32) with $E_s = 0$.

G. The Three-Temperature Model System of Equations

The model leads to a system of six equations in six unknowns: E_s, E_m, E_t, V, A, and R. The first equation is obtained from a total energy balance on dV, and is the equation for dV/dt. This is really the combination of equations (28), (30) and (32) as described in section F, above. Three more equations are obtained from the global energy balances described in section C, above. The remaining equations are the geometric relationships among volume, radius and area. These geometric relationships are summarized first, then the balance equations will be obtained. The system of balance equations is summarized in Table 1; the system of differential equations is summarized in Table 2.

1. Geometric Equations. For a free air burst, the fireball is spherical, so that:

$$A = 4\pi R^2 \qquad V = \frac{4}{3}\pi R^3 = A R / 3 \qquad (33)$$

It is worth noting at this point that none of the derivation of this model has been dependent on the assumption of spherical geometry. Therefore, if a ground burst were to be analyzed, it would only be necessary to assume that no energy is transferred into the ground and to replace equations (33) with those appropriate to the geometry considered.

2. Streaming Radiation Energy Balance. The global balance equation is:

(Streaming Energy at t') = (34)

(Streaming Energy at t)

\+ (Production from Yield during dt)

\- (Absorption inside fireball during dt)

\- (Transfer through surface at R during dt)

\+ (Streaming Energy present in dV at t')

From equation (8)

$$(\text{Streaming Energy at } t) = V E_s(t)$$

and similarly

$$(\text{Streaming Energy at } t') = V E_s(t')$$

Recalling equation (14)

$$(\text{Production from Yield during } dt) = Y f(t)\, dt$$

Defining the term dE_{sm} to be the energy density converted from streaming to material energy density during dt:

$$(\text{Absorption inside Fireball during } dt) = V_{ave}\, dE_{sm}$$

Recalling equation (24)

$$(\text{Transfer through surface at R during } dt) = c\, E_s\, A\, dt$$

Assuming the streaming energy density in dV at t' is the same as the streaming energy density in V at t (as was tacitly assumed in the derivation of dV/dt), then

$$\text{(Streaming Energy present in dV at t')} = E_s\, dV$$

Substitution of these expressions into equation (34) gives the desired balance equation:

$$E_s' V' = E_s V + Y f(t)\, dt - dE_{sm} V_{ave} - c E_s A\, dt + E_s\, dV \tag{35}$$

where:

$$\text{If } T_m = T_b \text{ and } [aT_m^4 - E_t] < E_s$$
$$\text{Then } dE_{sm} = C(T_m)\,[aT_m^4 - E_t]\, dt$$
$$\text{Otherwise } dE_{sm} = C(T_m)\, E_s\, dt \tag{36}$$

Then, since

$$\frac{d}{dt}(E_s V) = \lim_{dt \to 0} [E_s(t+dt)V(t+dt) - E_s(t)V(t)]/dt \tag{37}$$

Equation (35) implies:

$$\frac{d}{dt}(E_s V) = V\, dE_{sm}/dt + E_s \frac{dV}{dt} + Y f(t) - c E_s A \tag{38}$$

where

$$\text{If } T_m = T_b \text{ and } [aT_m^4 - E_t] < E_s$$
$$\text{Then } dE_{sm}/dt = C(T_m)\,[aT_m^4 - E_t]$$
$$\text{Otherwise } dE_{sm}/dt = C(T_m)\, E_s \tag{39}$$

3. Material Energy Balance. The global balance equation is:

(Material Energy at t') = (40)

(Material Energy at t)

\+ (Gain by absorption of radiation inside during dt)

\- (Loss by emission of radiation inside during dt)

\+ (Material Energy in dV at t')

Defining the term dE_{mt} to be the net energy density converted from material energy density to thermal radiation density during dt:

(Gain by absorption of thermal radiation inside during dt)

\- (Loss by emission inside during dt) (41)

$$= - dE_{mt} V_{ave}$$

Adding the gain by absorption of streaming radiation:

(Gain by absorption inside during dt)

\- (Loss by emission inside during dt) (42)

$$= V_{ave} (dE_{sm} - dE_{mt})$$

The other terms parallel those for streaming radiation, so the balance equation is:

$$E_m' V' = E_m V + V_{ave} (dE_{sm} - dE_{mt}) + E_m dV \quad (43)$$

where:

$$dE_{mt} = C(T_m)\,[aT_m^4 - E_t]\,dt \qquad (44)$$

which leads to the differential equation:

$$\frac{d}{dt}(VE_m) = V\,[dE_{sm}/dt - dE_{mt}/dt] + E_m\,\frac{dV}{dt} \qquad (45)$$

where:

$$dE_{mt}/dt = C(T_m)\,[aT_m^4 - E_t] \qquad (46)$$

4. Thermal Radiation Energy Balance. The global balance equation is:

$$\begin{aligned}\{\text{Thermal Radiation Energy at } t'\} &= \qquad (47)\\ &\{\text{Thermal Radiation Energy at } t\}\\ &+ \{\text{Production by emission inside during } dt\}\\ &- \{\text{Loss by absorption inside during } dt\}\\ &- \{\text{Transfer through surface at R during } dt\}\\ &+ \{\text{Thermal Radiation Energy present in } dV \text{ at } t'\}\end{aligned}$$

As was discussed in section F, above, there are two cases to consider here. If $dR/dt > c/4$, then the thermal radiation cannot enter dV in sufficient quantity to fill dV with thermal radiation of density E_t. It is therefore assumed that no conversion of thermal radiation to material energy

occurs in this case. As a result,

If $dR/dt > c/4$ then

$$\text{(Transfer through surface at R during dt)} = \text{(Thermal Radiation Energy present in dV at t')} \quad (48)$$

Otherwise

$$\text{(Transfer through surface at R during dt)} = \frac{c}{4} E_t A\, dt \quad (49)$$

$$\text{(Thermal Radiation Energy present in dV at t')} = E_t\, dV$$

Substituting equations (8), (41), (48) and (49) into (47) gives the global balance equation for thermal radiation:

If $dR/dt > c/4$

Then
$$E_t' V' = E_t V + dE_{mt} V_{ave} \quad (50)$$

Otherwise
$$E_t' V' = E_t V + dE_{mt} V_{ave} - \frac{c}{4} E_t A\, dt + E_t\, dV \quad (51)$$

Taking the limit as $dt \to 0$, and substituting equation (44) for dE_{mt}/dt gives the differential equations for the two cases:

If $dR/dt > c/4$

Then
$$\frac{d}{dt}(VE_t) = V C(T_m)\,[aT_m^4 - E_t] \quad (52)$$

Otherwise
$$\frac{d}{dt}(VE_t) = V C(T_m)\,[aT_m^4 - E_t] + E_t \frac{dV}{dt} - \frac{c}{4} E_t A \quad (53)$$

A numerical approach to solving these equation will be presented after considering the initial and final conditions for the solution.

H. Initial Conditions

The above system of equations is to be solved with the following initial conditions:

$$E_s = 0 \qquad E_t = 0 \qquad E_m = E_b$$
$$V = 0 \qquad \frac{dR}{dt} = c \tag{54}$$

Because the streaming radiation starts at a point, it has an initially infinite value, causing dR/dt = c.

I. Final Conditions

The three-temperature model applies until two conditions are both met: the streaming radiation has become negligible, and the material and thermal radiation energies are in equilibrium, i.e.:

$$\text{and} \qquad \begin{aligned} E_s &\approx 0 \\ T_m &\approx T_{eff} \end{aligned} \tag{55}$$

Once these conditions are met, the one-temperature model developed in the next section may be used.

TABLE 1

Three Temperature Model Balance Equations

$$A = 4\pi R^2 \qquad V = \frac{4}{3}\pi R^3 = A R / 3 \tag{33}$$

$$E_s' V' = E_s V + Y f(t)\, dt - dE_{sm} V_{ave} - c E_s A\, dt + E_s\, dV \tag{35}$$

$$E_m' V' = E_m V + V_{ave} (dE_{sm} - dE_{mt}) + E_m\, dV \tag{43}$$

If $dR/dt > c/4$ then

$$E_t' V' = E_t V + dE_{mt} V_{ave} \tag{50}$$

and

$$c E_s A\, dt = (E_s + E_m)\, dV \tag{27}$$

Otherwise

$$E_t' V' = E_t V + dE_{mt} V_{ave} - \frac{c}{4} E_t A\, dt + E_t\, dV \tag{51}$$

and

$$A (c E_s + \frac{c}{4} E_t)\, dt = (E_s + E_t + E_m)\, dV \tag{31}$$

Where:

$$dE_{mt} = C(T_m) [aT_m^4 - E_t]\, dt \tag{44}$$

and

If $T_m = T_b$ and $[aT_m^4 - E_t] < E_s$

Then $dE_{sm} = C(T_m) [aT_m^4 - E_t]\, dt$

Otherwise $dE_{sm} = C(T_m) E_s\, dt$ (36)

TABLE 2

Three Temperature Model Differential Equations

$$A = 4\pi R^2 \qquad V = \frac{4}{3}\pi R^3 = A R / 3 \tag{33}$$

$$\frac{d}{dt}(E_s V) = V\, dE_{sm}/dt + E_s \frac{dV}{dt} + Y f(t) - c E_s A \tag{38}$$

$$\frac{d}{dt}(VE_m) = V [dE_{sm}/dt - dE_{mt}/dt] + E_m \frac{dV}{dt} \tag{45}$$

If $dR/dt > c/4$ then

$$\frac{d}{dt}(VE_t) = V C(T_m) [aT_m^4 - E_t] \tag{52}$$

and

$$\frac{dV}{dt} = A c E_s / (E_s + E_m) \tag{28}$$

Otherwise

$$\frac{d}{dt}(VE_t) = V C(T_m) [aT_m^4 - E_t] + E_t \frac{dV}{dt} - \frac{c}{4} E_t A \tag{53}$$

and

$$\frac{dV}{dt} = A c (E_s + E_t/4) / (E_s + E_t + E_m) \tag{32}$$

Where:

$$dE_{mt}/dt = C(T_m) [aT_m^4 - E_t] \tag{46}$$

and

If $T_m = T_b$ and $[aT_m^4 - E_t] < E_s$

Then $dE_{sm}/dt = C(T_m) [aT_m^4 - E_t]$

Otherwise $dE_{sm}/dt = C(T_m) E_s$ (39)

J. Finite Differencing the Three-Temperature Model

This section describes an algorithm for solving the three-temperature model equations by finite differencing. A program implementing this method in Microsoft Basic version 5.2 is listed in Appendix B.

1. Evaluate dV.

a. Assuming streaming only, solve equation (27):

$$dV = c\ A\ dt\ E_s\ /\ (E_s + E_m) \tag{56}$$

b. Verify that dR/dt > c/4 using:

$$dR = 3\ dV\ /\ A \tag{57}$$

c. If dR < (c/4)dt then streaming and diffusion both contribute to fireball growth. Solve equation (31) for dV:

$$dV = c\ A\ dt\ (E_s + E_t/4)\ /\ (E_s + E_t + E_m) \tag{58}$$

d. The new volume is

$$V' = V + dV \tag{59}$$

2. Evaluate Energy Density Conversions. The conversion among energy densities is determined by equations (36) and (44) as follows:

a. Find the density converted from streaming to material energy, dE_{sm}, assuming it is not bounded by transparency of the air above T_b using equation (36):

$$dE_{sm} = C(T_m)\, E_s\, dt \tag{60}$$

b. Find the net density converted from material to thermal radiation energy, dE_{mt}, using equation (44):

$$dE_{mt} = C(T_m)\, [aT_m^4 - E_t]\, dt \tag{61}$$

c. If the fireball is at burnout, i.e. if $T_m = T_b$ then bound dE_{sm} by dE_{mt}, hence applying the conditional portion of equations (36). Thus:

$$\begin{aligned} &\text{If} && dE_{mt} < dE_{sm} \\ &\text{Then let} && dE_{sm} = dE_{mt} \end{aligned} \tag{62}$$

3. Solve Global Balance Equations for Energy Densities.

a. Find E_s' by solving the energy balance, equation (35), for E_s':

$$E_s' = E_s - dE_{sm}\, V_{ave}/V' + Yf(t)dt/V' - c\, E_s\, dt\, A/V' \tag{63}$$

b. Find E_m' by solving the energy balance, equation (43), for E_m':

$$E_m' = E_m + (dE_{sm} - dE_{mt})\, V_{ave} / V' \qquad (64)$$

c. Find E_t' by solving equation (50) or (51), depending on whether dR/dt > c/4 or not, respectively:

If dR/dt > c/4 then

$$E_t' = E_t\, V / V' + dE_{mt}\, V_{ave} / V' \qquad (65)$$

otherwise

$$E_t' = E_t + dE_{mt}\, V_{ave} / V' - \frac{c}{4} E_t\, dt\, A/V' \qquad (66)$$

4. Evaluate the Remaining Variables. Solve equations (6), (7), and (33) algebraically for T_m', T_{eff}', R', and A' in terms of E_m', E_t', and V', respectively. This completes the solution for one time step, so all that remains is to test against the stopping conditions presented in section IV.I, above, and iterate as required.

5. Initializing the Iterative Procedure. The initial conditions are presented in section IV.H, above. The iterative equations cannot have V = 0, however. This is avoided by using a first time step of size 2*dt, which, together with dR/dt = c gives a starting radius of:

$$R = 2\, c\, dt \qquad (67)$$

The volume and area corresponding to this radius are then calculated. Then, since $E_m(0) = E_b$ and $E_t(0) = 0$ a total energy balance is used to find E_s:

$$Y\ f(dt)\ 2\ dt = V\ [E_s + E_b] \qquad (68)$$

These values are then treated as initial conditions for the iterative algorithm.

6. Other Considerations. The iterative scheme described here implicitly assumes that $dV \ll V$ and $dR \ll R$. If a constant time step, dt, is used, then these conditions are not met for the early time steps. Equations (56), (57) and (58) for dV and for dR must be altered to include spherical divergence in these cases in order to achieve accurate results. In some places, formulas must be rearranged to avoid loss of precision from subtraction of nearly equal quantities, or to avoid fatal program errors (such as division by zero). The use of a first time step of 2 dt rather than dt avoids such problems during the second time step, for example. The program listed in Appendix B incorporates these requirements, and is annotated with remark statements where they occur.

V. Equilibrium Phase:
One-Temperature Homogeneous Model

A. Additional Assumptions

The assumptions required for the three-temperature model, detailed in section III above, are also required for the one-temperature model presented in this section. In addition, the one-temperature model assumes:

-- the yield pulse has been completed

-- the streaming radiation has been absorbed

-- the thermal radiation is in equilibrium with the material energy.

Under these conditions, the energy densities inside the fireball are characterized by a single temperature, T, defined by:

$$T_{eff} = T_m = T \qquad (69)$$

This equilibrium can never actually be reached, but it is approached closely. For example, 50 shakes after the start of a 20 kiloton burst of 10 shakes duration, the three-temperature model predicts that T_{eff} and T_m differ by 0.3%.

It is worth noting at this point that it is not possible to use the computer implementation of the three-temperature model beyond the point where equilibrium is (nearly) reached, because the numerical method becomes unstable. This difficulty is discussed in Appendix B.

Therefore, use of the one-temperature model is required in order to extend the computations to hydroseparation.

B. Approach to the Problem

The unknowns of the three-temperature model are T_{eff}, T_m, E_s, E_t, E_m, V, R, and A. The approach to the problem used here is to express all these unknowns in terms of a single parameter, T. Then a differential equation for T(t) in terms of physical constants, yield, and T, will be obtained. This equation can be solved for T(t) using conventional numerical techniques. All the desired unknowns can then be calculated from T.

C. Reduction to a Single Parameter: T

T_{eff}: from equation (69):

$$T_{eff} = T \tag{70}$$

T_m: from equation (69):

$$T_m = T \tag{71}$$

E_s: by assumption:

$$E_s = 0 \tag{72}$$

E_t: from equations (7) and (70):

$$E_t = aT^4 \tag{73}$$

E_m: from equations (6) and (71):

$$E_m = c_v T \tag{74}$$

V: since all the yield has been delivered:

$$V\ (E_s + E_t + E_m) = Y \tag{75}$$

Substituting equations (72) through (74) into (75):

$$V = \frac{Y}{aT^4 + c_v T} \tag{76}$$

R: assuming a spherical fireball:

$$R = (3\ V\ /\ 4\pi)^{1/3} \tag{77}$$

Substituting equation (76) for V:

$$R = \left[\frac{3\ Y}{4\pi\ (aT^4 + c_v T)}\right]^{1/3} \tag{78}$$

A: again, assuming a spherical fireball:

$$A = 3\ V\ /\ R \tag{79}$$

Substituting equations (76) and (78) into (79):

$$A = 3\ (4\pi/3)^{1/3} \left[\frac{Y}{aT^4 + c_v T}\right]^{2/3} \tag{80}$$

D. Differential Equation for T(t)

In order to develop a first-order, nonlinear, ordinary differential equation for T(t), it is noted that either V or T can be used as the independent parameter. Since equation (32) provides dV/dt, the relations developed in section C above can be used to convert to dT/dt.

Applying the chain rule to dV/dt:

$$\frac{dV}{dt} = \frac{dV}{dT}\,\frac{dT}{dt} \tag{81}$$

which can be solved for dT/dt. First, expressions for dV/dt and dV/dT in terms of T are derived.

Substituting equations (72), (73), (74), and (80) into equation (32):

$$\frac{dV}{dt} = \frac{3c}{4}\left(\frac{4\pi}{3}\right)^{1/3}\left[\frac{Y}{aT^4 + c_v T}\right]^{5/3}\frac{aT^4}{Y} \tag{82}$$

Differentiating equation (76) with respect to T:

$$\frac{dV}{dT} = \frac{-Y}{(aT^4 + c_v T)^2}\left(\frac{4aT^4 + c_v T}{T}\right) \tag{83}$$

Solving equation (81) for dT/dt and substituting equations (82) and (83) gives the desired result:

$$\frac{dT}{dt} = -\frac{3c}{4}\left[\frac{4\pi}{3}\,\frac{(aT^4 + c_v T)}{Y}\right]^{1/3}\left(\frac{aT^4}{4aT^4 + c_v T}\right)T \tag{84}$$

E. Initial and Final Conditions

The initial conditions for the one-temperature model are the same as the final conditions for the three-temperature model. The final condition for the one-temperature model is hydroseparation, which occurs when the rate of growth of the fireball has fallen sufficiently for the acoustic velocity in the fireball to equal dR/dt. This occurs at about 300,000 C, i.e. about 25 eV [Ref 1:65]. Examples computed using this model are presented in the next section. The endpoint for these computations is taken to be T = 25 eV. More detailed consideration of the conditions for hydroseparation is a question of hydrodynamics and is outside the scope of this thesis.

VI. Numerical Results

This section presents graphs of the temperatures, radii, and growth rates predicted by the homogeneous (three-temperature, then one-temperature) model. The results of the early time model are shown for comparison. The homogeneous model results are drawn as solid lines and the early time model as dashed lines in figures 4 through 7, below. These results are for a 20 kiloton burst, in sea level air, with a square yield pulse of 5.14493 shakes duration. The curves labeled "f(t)" are included to indicate the shape and duration of the yield pulse, but have been rescaled in height for convenient display, and thus are not normalized to unit area as is the actual f(t).

Observations regarding the important features of these curves are made in this section. An evaluation of the model based on these observations is presented in the following section.

A. Material and Thermal Radiation Temperatures

Figure 4 shows T_m and T_{eff} for 20 shakes. Important features of this graph include:

-- T_{eff} is a smoothly varying function of time

-- T_m stays at T_b only briefly, but is held out of equilibrium until the end of the yield pulse

-- $T_m > T_{eff}$ at all times

-- The early rise of T_{eff} is essentially the same for both models, and the early time model falls rapidly down to the level of the homogeneous model after the yield pulse ends.

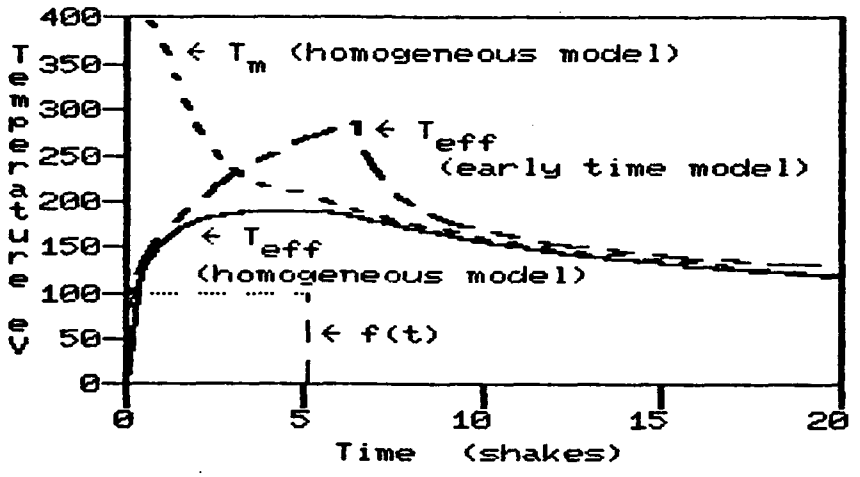

Fig. 4 Temperature Comparison, 20KT

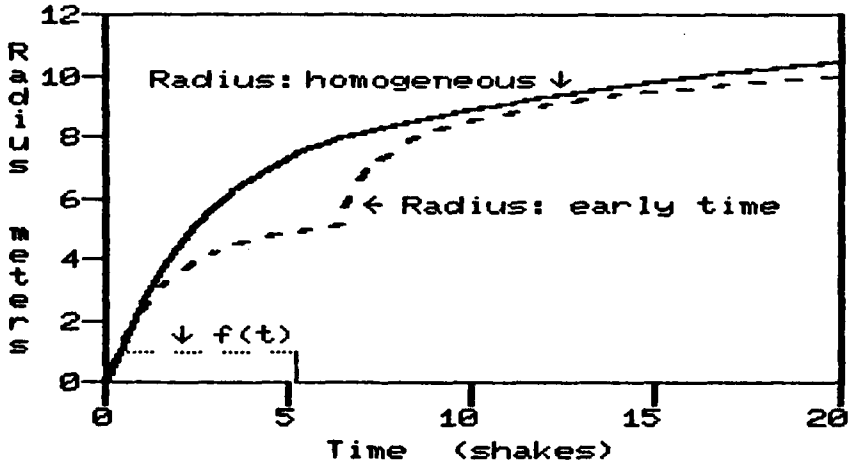

Fig. 5 Radius Comparison, 20KT

B. Radius

Figure 5 shows the radius as a function of time for 20 shakes as predicted by the two models. Important features include:

-- The homogeneous model radius is a smoothly varying function of time

-- The early time model radius converges upon the homogeneous model radius within about 5 shakes after the yield pulse ends

-- The models are very similar at the beginning of the yield pulse.

C. Growth Rate

Figure 6 shows the growth rate, dR/dt, of the two models for 20 shakes. Important features of the homogeneous model growth rate include:

-- smoothly varying function of time

-- monotone decreasing

-- never exceeds the speed of light

-- decreases as streaming radiation is lost after the yield pulse ends.

-- The early time model predicts about the same growth rate once the spike to values greater than c decays.

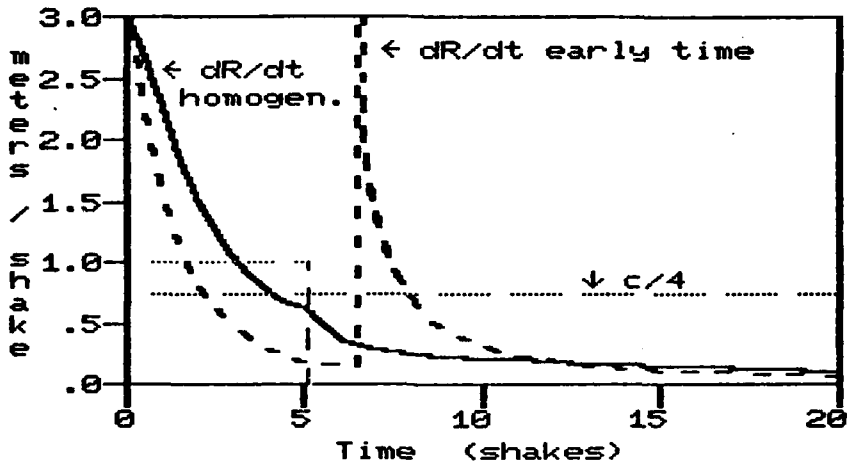

Fig. 6 Growth Rate Comparison, 20KT

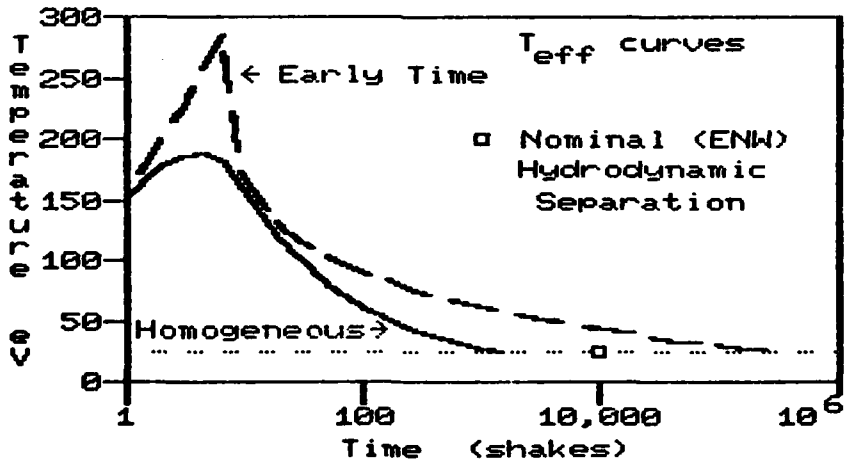

Fig. 7 Hydrodynamic Separation Comparison with Nominal

D. Hydrodynamic Separation

Hydrodynamic separation should be predicted to occur when a temperature of 300,000^{0}C, i.e. 25 eV, is reached, at a time of about 0.1 millisecond, i.e. about 10^{4} shakes, for a 20KT burst [Ref 1.65]. Figure 7 is a semi-log graph of T_{eff} for both models, with each extended until it predicts hydrodynamic separation. The nominal case described above refers to a total yield of 20 kilotons, for an x-ray yield of about 15 kilotons. The curves are for an x-ray yield of 20 kilotons, but the difference in predicted hydrodynamic separation times is negligible because of the steep decrease at the left of the (semi-log) curves.

The homogeneous model predicts 25 eV at 1500 shakes, which is a factor of 6.7 underestimate compared to 10,000 shakes. The early time model, however, predicts 364,000 shakes, which is a factor of 36.4 overestimate.

E. Other Comparisons

Appendix A presents graphs for 1 kiloton and 4 megaton yields and for various pulse shapes and durations, and discusses some of the conclusions which may be drawn from them. The features seen above are common to all the various yields and pulse shapes.

The major characteristics of the models observed from these comparisons are:

— The results predicted by the homogeneous model are very insensitive to the pulse shape and duration, so long as the pulse duration is short compared to the yield (2 shakes at 1KT, 10 shakes at 4MT).

— The results predicted by the early time model, specifically, the height and time of the peaking of T_{eff} is sensitive to the pulse shape and duration, even for short duration pulses.

Appendix C develops a modified version of the homogeneous model which accounts for spherical divergence of the streaming radiation. Graphical comparisons to both the homogeneous model and the early time model are shown. The significant observation drawn from those comparisons is that the modified (divergent) model gives essentially the same results as the unmodified (homogeneous) model.

VII. Evaluation of the Homogeneous Model

This section evaluates the homogeneous model by consideration of those features which were found (in section II) to be problems with the early time model. Predictive and pedagogical advantages will each be discussed, followed by a consideration of some limitations of the model, and of its potential for growth into a more sophisticated model.

A. Predictive Advantages of the Homogeneous Model

1. Effective Temperature. T_{eff} is a smoothly varying function of time, as would reasonably be expected. The overall shape and numerical values are in agreement with the early time model, but with the peaking (at the transition from burnout to diffusion) smoothed out. This is a result of allowing T_m to fall below T_b independently of the transition from streaming to diffusion, and of accounting for simultaneous transport by streaming and diffusion both.

2. Decreasing Fireball Expansion Rate. dR/dt is a monotone decreasing function of time with, in particular, a decrease after the yield pulse ends due to loss of transport by streaming (which is four times more efficient than transport by diffusion). The reasons for this improvement are the same as those noted in the previous paragraph.

3. Constraint by the Speed of Light. The expansion rate of the fireball never exceeds the speed of light, unlike the expansion rate predicted by the early time model. The reason for this improvement is that the growth rate is modeled by consideration of the conditions at the boundary, using a local energy balance. Since energy density flows through the surface at a maximum speed of c, and the energy density accumulated in dV is greater than that entering through the surface, then the growth rate is inevitably less than c.

4. T_m versus T_{eff} The material temperature, T_m, always exceeds the effective thermal radiation temperature, T_{eff}, as is required by physical considerations. The homogeneous model is successful in predicting this result because it does not decrease E_m by dilution (as do the moment equations of the early time model) but rather it explicitly models the conversion of E_t to E_m by absorption in the surface absorption layer of ambient air.

B. Pedagogical Advantages

1. No Integrals over Retarded Time. The homogeneous model avoids the confusion of retarded time and the complexities of visualization of the interaction processes as modeled by integrals over retarded time.

2. No Moments Equations. The homogeneous model avoids the abstract and physically unconvincing use of moments equations obtained from the diffusion equation.

3. Derived by Local and Global Energy Balances. The three-temperature homogeneous model is derived using only energy balances and geometric relationships. Each term in the balance equations can be interpreted as describing an individual process of physical significance. This approach engenders the sense of intuitive, physical understanding which is prerequisite to the application of more sophisticated techniques, and which is the pedagogical objective.

4. Easily Computerized. The homogeneous model leads directly to a simple finite differencing scheme (essentially, a forward Euler scheme). This scheme can be programmed and run on personal computers (which is becoming an increasingly important resource as more students obtain them). Doing so is a task of appropriate size to be assigned as an exercise or project.

5. Reasonable Numerical Results. The results obtained from the computer exercise suggested above are numerically reasonable, both in terms of curve shapes and physical constraints, and in terms of the actual numbers computed.

C. Limitations of the Homogeneous Model

The accuracy of the model is limited by that of the assumptions made in its development. These assumptions are of two kinds, assumptions about the physical parameters of the air, e.g. heat capacity as a function of temperature, and assumptions about the distribution and transport of energy in the fireball.

The limitations imposed by assumptions about the physical parameters are not of great conceptual significance. If, for example, the assumption of constant heat capacity were revised to an assumption of some particular temperature dependence, the computer program would be changed only by the introduction of a subroutine to evaluate the heat capacity, and the numerical results would change. The general shape of the resulting curves would be unchanged, as long as a reasonable $C_v(T)$ was chosen, and the same physical constraints ($dR/dt < c$, etc.) would be met.

The limitations imposed by assumptions about the distribution and transport of energy are of conceptual importance, for it is these assumptions which constitute the model. The assumption of uniform spatial distribution of thermal radiation is justified by the fact that the fireball is optically thin. The thermal radiation then tends to closely couple the material energy in different regions of the fireball, so that it is reasonable to assume that the material temperature is uniformly distributed.

The assumption that the streaming radiation energy density, E_s, is also uniformly distributed in the fireball must be recognized as the major conceptual limitation of the model. By its very nature as streaming radiation, E_s must be spherically divergent, and so cannot be uniformly distributed. On the other hand, its distribution also depends on the yield rate function, f(t), which leads to considerations of retarded time. The reason the assumption was made was to eliminate retarded time from the model. The assumption can be justified, to a certain extent, by the fact that it results in reasonably good numerical predictions.

The assumption of spatially uniform E_s can actually be replaced by taking the more general view that E_s has some (non-uniform) distribution within the fireball, but that its interaction rates can be characterized by its average value within the fireball. This average value can then be computed using a global energy balance. The important limitation is then introduced by the assumption that the flux of streaming radiation at the surface, $c\,E_s(R,t)$, can be computed by using the average E_s as an approximation for the surface value: $c\,E_s(R,t) \simeq c\,E_s(t)$ From this viewpoint, the limitation is one of making a first-order approximation rather than a physically unreasonable assumption.

Appendix C develops a modified homogeneous model which assumes that the streaming radiation is spherically divergent, and hence distributed as $1/r^2$. This ignores the effects of absorption and emission histories on the distribution. The resulting approximation is that

$$E_s(R,t) \approx \frac{1}{3} E_s^{(ave)}(t) \qquad (85)$$

This modification causes only small changes in the predicted temperatures and radii, indicating that the homogeneous model is insensitive to the distribution of streaming radiation, whatever it may be. This helps explain how such a simple model gives good numerical results.

D. Extension to More Sophisticated Models

Three approaches to obtaining better numerical results suggest themselves: better input data, a more elegant model, and brute force application of the model.

Better input data would consist of using detailed data on the variation of the physical parameters with temperature, as was discussed above.

A more elegant model could be obtained by assuming some non-uniform spatial distribution for one or more of the energy densities, and using it to obtain a higher order approximation for the surface conditions (which determine dR/dt) in terms of the average conditions (which are

determined by the global energy balances). Appendix C presents an example of this approach.

The homogeneous model presented here could be extended by brute force to include radial variations in temperatures and energy densities. This could be done by treating the fireball as a collection of concentric spherical shells. Each shell would be thin, so the homogeneous model would apply. The boundaries among shells could be treated using the same methods as are applied at the surface of the fireball in the homogeneous model, that is , the same modeling of the equilibration and transport processes. Such a model could be extended past hydrodynamic separation by treating the shells as Eulerian coordinate cells for hydrodynamic transport simultaneously with the radiative transport model developed here.

VIII. Conclusions and Recommendations

A. Pedagogical Use of the Homogeneous Model

The goal of this research was to develop and evaluate a model of the radiative growth phase of fireball growth, comparing it to G. C. Pomraning's early time model [Ref 2]. The model sought was intended for pedagogical use. It was therefore to be based on simple models of the relevant physical processes and to provide physically and numerically reasonable results. The three-temperature homogeneous model, together with its one-temperature simplifications (for application after thermal equilibrium is closely approached) has been developed and shown to be such a model. It is recommended for pedagogical use.

B. Computational Use of the Homogeneous Model

It has further been shown that this homogeneous model gives numerical results which are more reasonable in meeting necessary physical constraints than those results obtained from the early time model. Specifically, the growth rate of the fireball is monotone decreasing and always less than the speed of light, as predicted by the homogeneous model, and the effective thermal radiation temperature is predicted to be a smooth function of time. Overall, however, the

homogeneous model predicts temperatures and radii which are quite comparable to those predicted by the early time model. The homogeneous model has the additional advantage of computational simplicity relative to the early time model. It is concluded that the homogeneous model is a useful computational method of at least first-order accuracy. It is recommended that its results be compared with those of a state-of-the-art production code to evaluate its actual accuracy with greater confidence.

C. The Homogeneous Model as a Basis for More Sophisticated Models

The simple models of radiative emission, absorption, and transport used in the homogeneous model give surprisingly good numerical results. These models could be applied to a discrete ordinates method to obtain more accuracy in the radiative stage of fireball growth. The discrete ordinates code obtained could then be combined with an Eulerian hydrodynamics code to obtain a radiative hydrodynamics model for the later stages of fireball growth. These approaches are recommended for consideration.

Bibliography

1. Glasstone, S. and P. J. Dolan. The Effects of Nuclear Weapons (Third edition). Washington, D. C.: United States Government Printing Office, 1977.

2. Pomraning, G. C. "Early Time Air Fireball Model for Near Surface Energy Release," Nuclear Science and Engineering,53: 220-225 (1974).

3. Pomraning, G. C. Early Time Air Fireball Model for a Near-Surface Burst. Science Applications, Inc., La Jolla, Ca., report under Defense Nuclear Agency contract DNA001-73-C-0012. Defense Nuclear Agency publication DNA3029T (SAI-72-588-LJ), March, 1973.

4. U.S. Standard Atmosphere. National Oceanographic and Atmospheric Administration publication S/T76-1562. Washington, D. C.: United States Government Printing Office, 1976.

Appendix A

Comparison of Results of the Two Models

This appendix presents graphs of the temperatures predicted by the early time model and the homogeneous model. The examples presented include yields of one kiloton and four megatons, with three cases of yield pulse (shape and duration) for each yield.

One Kiloton Examples

Figure A-1 shows the three yield pulses considered for the one kiloton examples and indicates the choice of line or dash used to indicate each case in the subsequent figures. Figure A-2 shows the effective radiation temperatures for the three cases as predicted by the early time model. The temperatures as predicted by the homogeneous model for these same cases are shown in figure A-3 . Conclusions which may be drawn from these figures are:

-- the homogeneous model predicts a longer, lower temperature curve for a longer, lower yield pulse, whereas

-- the early time model predicts a longer, higher temperature curve for a longer, lower yield pulse;

-- the homogeneous model predictions are insensitive to yield pulse shape as long as the pulse is short (in comparison to the total yield), whereas

-- the early time model predicts a peaking of T_{eff}, the timing of which is sensitive to pulse shape.

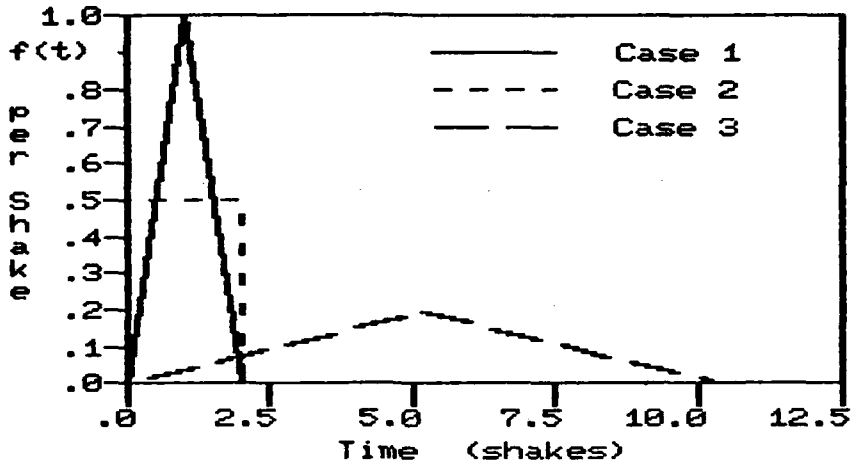

Fig. A-1 Yield Pulses for 1 Kiloton Examples

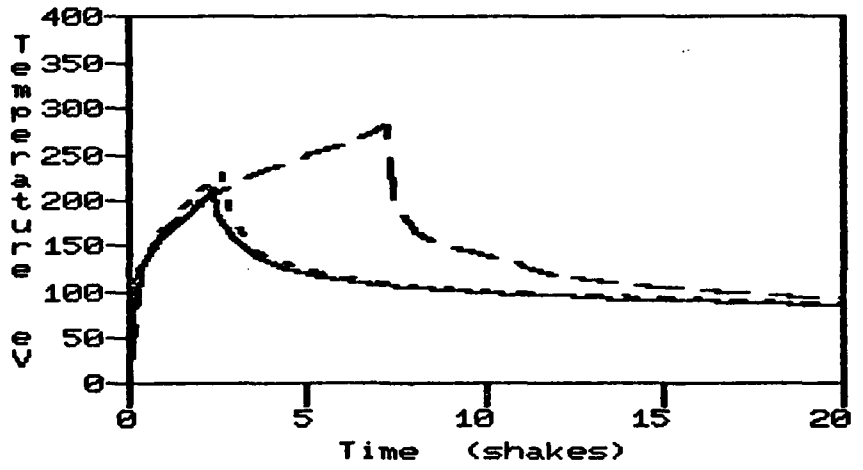

Fig. A-2 Early Time Model T_{eff} for 1 Kiloton Yield

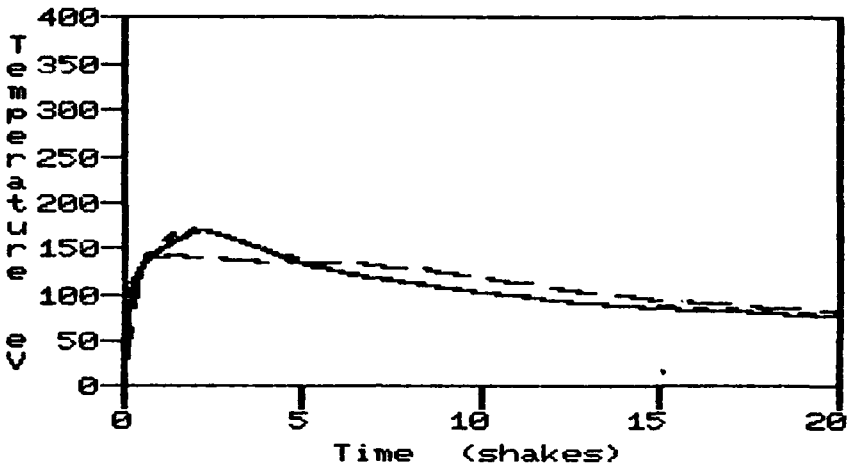

Fig. A-3 Homogeneous Model T_{eff} for 1 Kiloton Yield

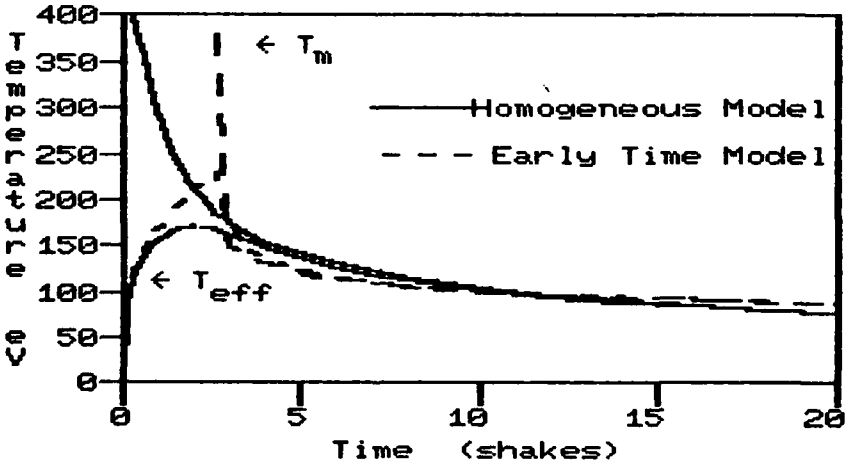

Fig. A-4 Temperatures for Both Models

with 2 Shake, Square Pulse of 1 Kiloton Yield

For direct comparison of the two models, including the material temperature, figure A-4 presents both T_m and T_{eff} for the one kiloton yield. The yield pulse for this example is case 2, the square pulse of 2 shakes duration. This comparison demonstrates the good general agreement of the two models.

Four Megaton Examples

Figure A-5 shows the three yield pulses considered for the four megaton examples and indicates the choice of line or dash used to indicate each case in the subsequent figures. Figure A-6 shows the effective radiation temperatures for the three cases as predicted by the early time model; figure A-7 is an expanded view of this same information. The temperatures as predicted by the homogeneous model for these same cases are shown in figure A-8. The three curves in this figure are essentially identical. Conclusions which may be drawn from these figures are:

-- the homogeneous model is very insensitive to pulse shape and duration for this large yield, whereas

-- the early time model still predicts a higher, longer T_{eff} pulse for a longer, lower yield pulse.

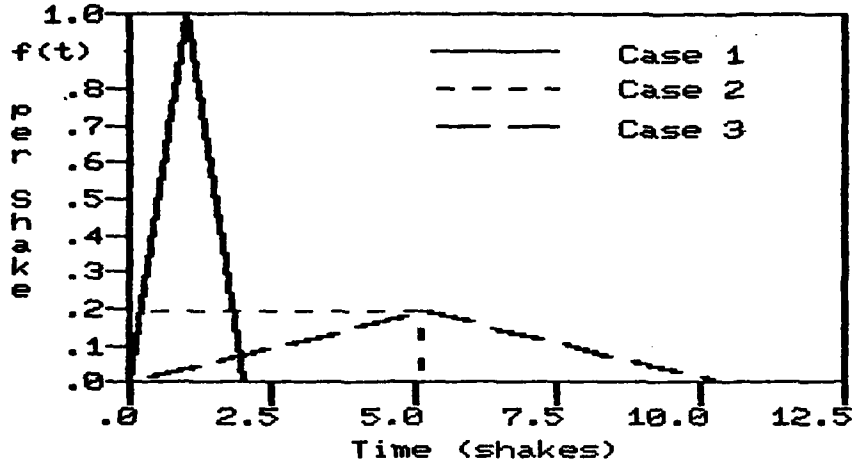

Fig. A-5 Yield Pulses for 4 Megaton Examples

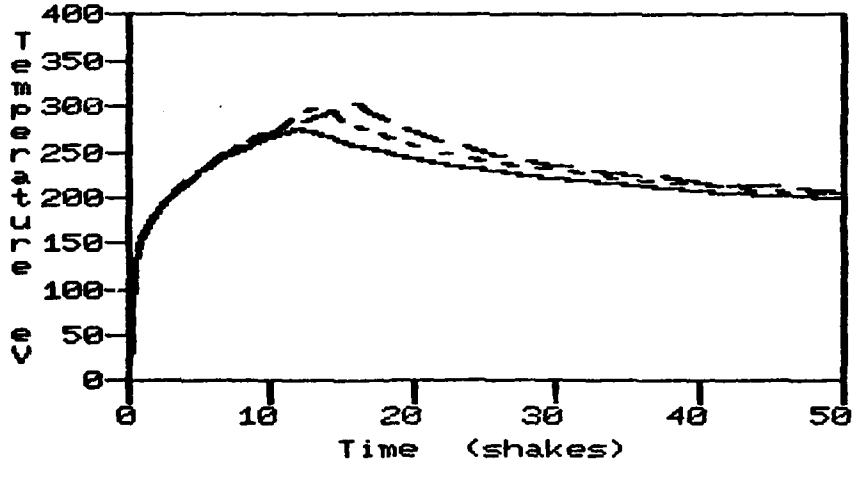

Fig. A-6 Early Time Model T_{eff} for 4 Megaton Yield

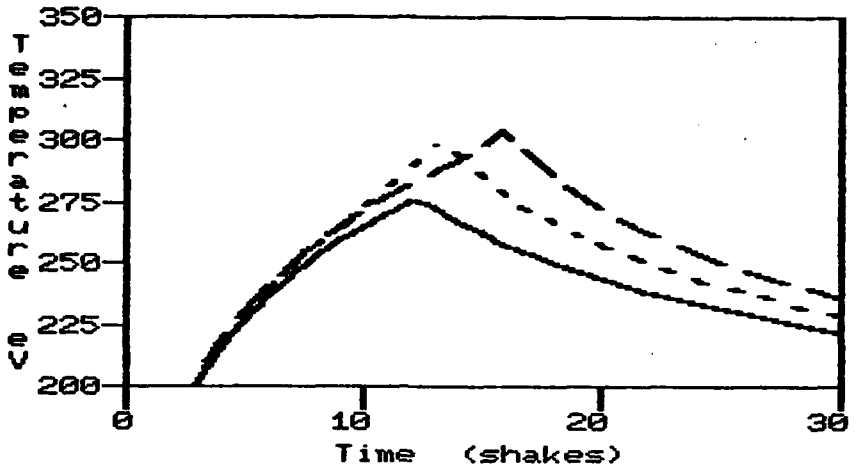

Fig. A-7 Expanded View of Early Time Model T_{eff}

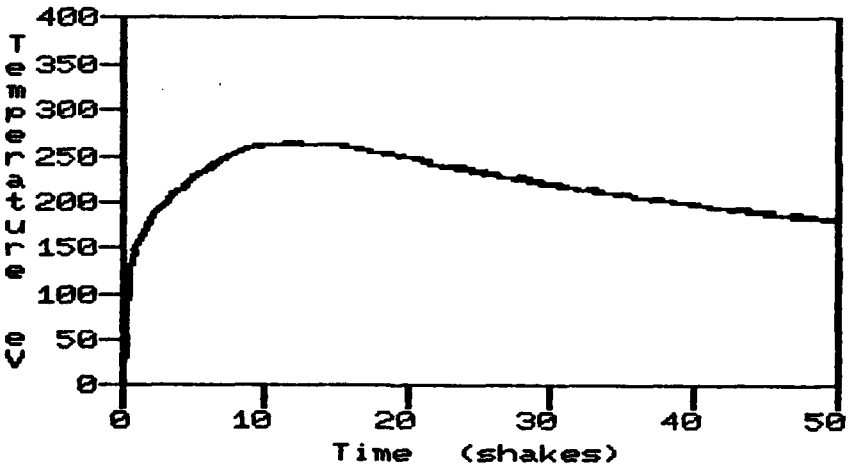

Fig. A-8 Homogeneous Model T_{eff} for 4 Megaton Yield

For direct comparison of the two models, including the material temperature, figure A-9 presents both T_m and T_{eff} for the four megaton yield. The yield pulse for this example is case 2, the square pulse of 5.14493 shakes duration. This comparison again demonstrates the good general agreement of the two models.

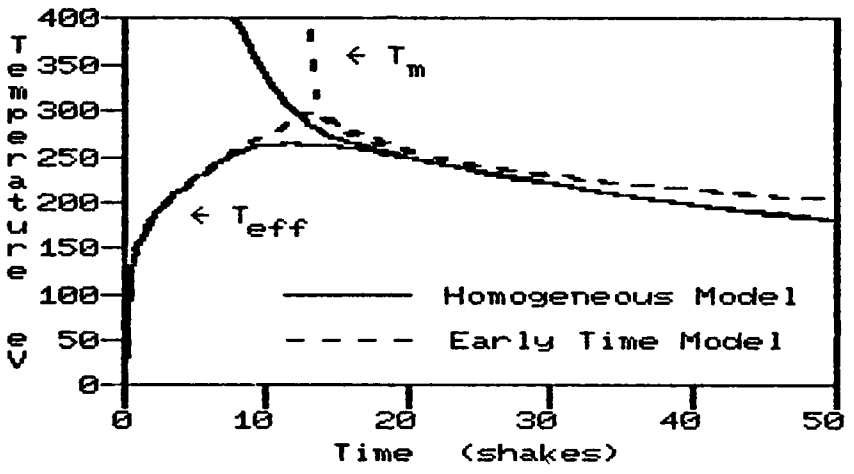

Fig. A-9 Temperatures for Both Models

with 5.14493 Shake, Square Pulse of 4 Megaton Yield

Appendix B

Basic Computer Program

for

Three-Temperature Homogeneous Model

```
10 'Radiative phase fireball growth program
20 '  based on three-temperature homogeneous model
30 '  by LCDR K. A. Mathews
40 '  for M.S. Thesis at Air Force Institute of Technology
50 WIDTH LPRINT 80  'Set Line Printer Line Width
60 DEFINT I-N   'Set Fortran-like Integer variable naming
70 DEF FNCOEF(T) =
          RHO.KAPPA.C * (T.B/T.M) * (T.B/T.M) * (T.B/T.M)
     'function call for temp. variation of kappa
80 DATA 8.9217E-2, 13.7, 400, 3, 3.14159, 4.96E10, 1.24E8
90 READ RHO.KAPPA.C, A, T.B, C, PI, E.B, C.V

100 'Enter problem parameters interactively
110 HOME:VTAB 2
120 PRINT "Enter parameters for square wave yield function:"
130 PRINT
140 HTAB 10: INPUT "Pulse width (shakes) = ",T.PULSE
150 PRINT: PRINT
160 PRINT "Enter Burst Parameters:": PRINT
170 HTAB 10: INPUT "Yield (kiloton) = ", YIELD
180 YIELD = YIELD * 4.2E+12  'Convert kilotons to Joules
190 YDOT = YIELD / T.PULSE   'Constant ydot for square pulse
```

```
200 PRINT: PRINT "Enter Quadrature Parameters:": PRINT
210 HTAB 10: INPUT "Time Increment (shakes) = ", DELTA.T#
220 DT = DELTA.T#  '# indicates double precision variable
     Time is carried in double precision for convenience in
     assuring output times round to desired times in
     printout
230 PRINT: HTAB 10
240 INPUT "Number of steps per printout = ", N.PRINT
250 PRINT: HTAB 10
260 INPUT "Max Time to which to compute: T.quit = ",T.QUIT
270 PRINT: PRINT "Commencing computations"
280 GOTO 400  'to initialize variables

300 'Data Lprint Subroutine
310 LPRINT T, V, R, R.DOT
     'Time, Volume, Radius, dR/dt
320 T.EFF = SQR (SQR (E.T / A) )
     'Computed here instead of in main routine to improve
     program speed of execution; T.eff is not needed for
     computations, only for data output
330 LPRINT E.S, E.M, E.T, T.M, T.EFF
340 LPRINT
350 RETURN
```

```
400 'Initialization of variables
410 T = 0: T# = 0
420 E.S = 0  'will be reinitialized by special first time
             step, as will E.m; all are set to zero first
             for benefit of initial printout
430 E.M = 0
440 E.T = 0
450 T.M = 0
460 T.EFF = 0
470 V = 0
490 R = 0
500 R.DOT = C

600 'Initial printout
610 LPRINT "Radiative Phase Fireball Growth Program:"
620 LPRINT
"      Version 4.3  --  Single Precision, No Ground Effects"
630 LPRINT "YIELD (KT) = "; YIELD/4.2E+12  'divide to get KT
640 LPRINT: LPRINT "Pulse Shape Parameters:"
650 LPRINT
"   Square Wave Pulse, starts at t = 0, ends at t ="; T.PULSE
660 LPRINT "   Yield Rate (J/shake) ="; YDOT
670 LPRINT: LPRINT "Quadrature Parameters:"
680 LPRINT "   Time Increment (shake) = "; DT
690 LPRINT "   Number per printout    = "; N.PRINT
700 LPRINT: LPRINT  'space printout then print data titles
```

```
710 LPRINT: LPRINT
     "T (shake)","V (m^3)","Radius (m)","dR/dt (m/shake)"
720 LPRINT "E.s (J/m^3)","E.m (J/m^3)",
                "E.th (J/m^3)","T.m (eV)","T.eff (eV)"
730 LPRINT
740 GOSUB 300 'Lprint initial conditions under the headings


800 'First Time Step: inner bdy = outer bdy at t = 0
    so special case. Go two time steps at once using
     dR/dt = c  to determine volume, and volume and yield
     to determine E.s
810 T = 2 * DT: T# = 2 * DELTA.T#: I = 2
820 T.M = T.B
830 E.M = E.B  'Assume Burnout because of high E.s due to
                small volume
840 R = C * T
850 V = 4 * PI * R * R * R / 3
860 IF T<T.PULSE
      THEN E.S = YDOT * T / V  - E.M
      ELSE E.S = YIELD / V - E.M
          'Yield by time 2*dt is ydot * t unless pulse is
          already over, then it is yield
870 E.T = 0     'Assume no buildup in short time 2*dt
880 R.DOT = C
900 GOSUB 300 'Data Printout to allow manual evaluation
     of reasonableness of first step, then start main loop
```

```
1000 'Main Iteration Routine
1010 'Energy Transformations in old volume V
1020 IF T.M = T.B
       THEN RHO.KAPPA.C.OF.T = RHO.KAPPA.C
       ELSE RHO.KAPPA.C.OF.T = FNCOEF(T.M)
     'Avoid calculating (T.b/T.b) cubed = 1 (for speed)
1030 DE.SM = RHO.KAPPA.C.OF.T * E.S * DT
     'This is potential amount to be absorbed, it will be
          bounded by amount required to maintain burnout
          if appropriate
1040 DE.MT = RHO.KAPPA.C.OF.T *
                (A * T.M * T.M * T.M * T.M - E.T) * DT
1050 IF T.M => T.B AND DE.MT =< DE.SM
       THEN DE.SM = DE.MT
   'Bounding if at burnout to prevent raising T.m above T.b
1100 'Find Volume elements for radiative transfer
     through surface in dt. The energy transferred is
     that present in a shell of thickness dr=c*dt (streaming)
     or r=(c/4)*dt (diffusion), extending inward from the
     surface of the fireball. If the shell is thick,
     its volume is V - Vol(interior to shell)
     (actually, this is always true), but if the shell is
     thin, this leads to errors in the subtraction, so
     its volume is computed as 4*pi*R^2*dr.
```

```
1110 IF C * DT < .001 * R  THEN GOTO 1170
1120 RS = R - C * DT
1130 RT = R - C * DT / 4
1140 DVS = V - 4 * PI * RS * RS * RS / 3
1150 DVT = V - 4 * PI * RT * RT * RT / 3
1160 GOTO 1200
1170 DVS = 4 * PI * R * R * C * DT
1180 DVT = PI * R * R * C * DT


1200 'Assume streaming only causes dR/dt,
     compare to c/4 to verify assumption
1210 DV = DVS * E.S / (E.S + E.M)
1220 V.NXT = V + DV
1230 R.NXT = (.75 * V.NXT / PI) ^ (1/3)
1240 R.DOT = (R.NXT - R) / DT
1250 IF R.DOT >= C/4
       THEN DVT = DV: GOTO 1400
     'Assumption correct, set dvt to dv so thermal
     does not contribute to E.m in growth volume,
     but E.t is decreased by dilution
```

```
1300 'Otherwise, recompute v.nxt, etc., to include thermal
     diffusion in growth, and recompute needed parameters
1310 DV = (DVS * E.S + DVT * E.T) / (E.S + E.T + E.M)
1320 V.NXT = V + DV
1330 R.NXT = (.75 * V.NXT / PI) ^ (1/3)
1340 R.DOT = (R.NXT - R) / DT

1400 'Energy balances on new volume for each of the energies
1420 DILUTED = (V+DV/2) / V.NXT
1430 IF T>T.PULSE   THEN DE.S.YIELD = 0
     ELSE IF T+DT < T.PULSE
          THEN DE.S.YIELD = YDOT * DT / V.NXT
     ELSE DE.S.YIELD = YDOT * (T.PULSE - T) / V.NXT
 'Compute addition to E.s based on yield delivered during dt
1440 E.S = E.S * (1 - DVS/V.NXT)
                   - DE.SM * DILUTED + DE.S.YIELD
1450 E.M = E.M + (DE.SM - DE.MT) * DILUTED
1460 E.T = E.T * (1 - DVT/V.NXT) + DE.MT * DILUTED

1500 'Set variables to next values
1520 V = V.NXT
1530 R = R.NXT
1540 T# = T# + DELTA.T#
1550 T = T#
1560 T.M = E.M / C.V
1570 I = I + 1
```

```
1600 'End-of-Phase Criteria checks
1610 IF T.M <= 25 OR T >= T.QUIT
       THEN GOSUB 300: GOTO 1700   'Line Print final data
1620 'Printout Criteria Check
1630 IF (I MOD N.PRINT) = 0
       THEN I = 0: GOSUB 300
   'reset I to zero to avoid overflow of integer data type
1640 GOTO 1000 'Loop to next iteration

1700 'End of Radiative only fireball growth.
     Hydroseparation assumed to occur at temp of 25 eV
     unless T.quit is reached first
1710 LPRINT CHR$(12) 'Form Feed
1720 GOTO 110  'Loop to parameter input routine for next
                problem.
```

Notes:

-- Everything on a numbered line subsequent to a ' is a remark and is ignored by the interpreter and compiler.

-- Multiple executable statements on a single numbered line are separated by colons

-- LPRINT prints on the line printer; PRINT writes to the display screen

-- This listing follows the syntax of BASIC-80, revision 5.2 for the Apple IIC Computer with Z-80 auxiliary processor, and is compatible with both the interpreter and compiler for that language, as distributed by Microsoft.

-- Stability of the Algorithm:

This algorithm is only conditionally stable. As equilibrium is approached, the time increment, dt, must be decreased to maintain stability. However, as dt is decreased, the subtractions in lines 1440 through 1460 introduce rounding error inaccuracies. Increasing the floating point word length, such as by using double precision, only delays the loss of accuracy, allowing a shorter dt. The solution to the difficulty is to use this program to the point of instability, and inspect the results to find reliable data on the approach to equilibrium. These results are then used as the initial conditions for the numerical integration of the one-temperature differential equation for T(t). Use of single precision (32 bit) floating point arithmetic for the combined model readily provides numerical results with enough significant digits for a tolerance of less than 1 eV. This method was used in computing the examples presented in this thesis.

Appendix C

Modification of the Homogeneous Model to Include Spherical Divergence of the Streaming Radiation

Objectives

The objective of the main body of this thesis has been to present the simplest possible model for the radiative growth phase of fireball formation in an atmospheric nuclear burst. As discussed in section VII.C, a significant limitation of the homogeneous model is its assumption of a uniform density of streaming radiation. This assumption seems unreasonable because of the $1/r^2$ radial attenuation caused by the spherical divergence implicit in the nature of the streaming radiation (as streaming from a point source). This appendix will develop the modifications to the homogeneous model to include this $1/r^2$ radial attenuation.

Factors Affecting Radial Distribution of E_s

There are actually three factors which affect the radial distribution of streaming radiation at any fixed instant of time, t, of which divergence is only one. The other two are the yield history which resulted in the emission of streaming radiation present at time t and the absorption to which the radiation at each radius has been subjected in reaching that radius by time t. To include

these latter two effects would require explicit use of retarded time and integrations over retarded time, as is done in the early time model. The objective of this appendix, however, will be to isolate the effects of divergence from those of emission history and absorption history, and hence avoid the use of retarded time.

Assumptions of the Divergent Model

In avoiding the use of retarded time, the divergent model (as the modified model will be called) assumes that absorption is negligible with respect to divergence in determining the radial distribution of the streaming radiation, and that the yield rate has been approximately constant over the interval in which the streaming radiation present at any time t was emitted. These conditions are effectively met during the emission period of a square-shaped yield pulse of short duration relative to the total yield. For this reason, the divergent model will be evaluated for three example cases, a one kiloton burst with a 2 shake square pulse, and twenty kiloton and four megaton bursts with a 5.14493 shake square pulse. These choices also allow comparison with the examples presented in sections II and VI and in Appendix A.

Method

The viewpoint suggested in section VII.C will be taken. Thus, the interactions of material and radiations inside the fireball are assumed to be characterized by the average values of the energy densities, E_s, E_m, and E_t. The interactions at the surface (in the thin absorption layer at the surface) of the fireball will be determined by the average values for the material and thermal energies, but by the surface value for streaming radiation, $E_s(R)$. This surface value is proportional to the average value with a proportionality constant which is to be determined by the assumption that $E_s(r) \sim 1/r^2$.

Derivation of $E_s(R)$ as a Function of E_s

Using the assumption of $1/r^2$ attenuation, let the constant B (possibly a function of time) be defined by:

$$E_s(r) = B / r^2 \qquad \text{(C-1)}$$

Then, the average value of the streaming radiation density is evaluated by:

$$E_s = \int_0^R E_s(r)\, 4\pi r^2\, dr / V$$

$$= \int_0^R \frac{B}{r^2}\, 4\pi r^2\, dr / V$$

$$= 4\pi R B / (4\pi R^3/3) = 3 B / R^2 \qquad \text{(C-2)}$$

But, evaluating equation C-1 at r=R and solving for B:

$$B = R^2 E_s(R) \qquad \text{(C-3)}$$

Substituting equation C-3 into equation C-2 gives the desired result:

$$E_s(R) = E_s / 3 \qquad \text{(C-4)}$$

Modified Balance and Differential Equations

To obtain the divergent model, all that is required is to substitute $E_s/3$ for E_s in the local and global balance equations in those terms representing interactions at the surface of the fireball. Thus, the three-temperature homogeneous balance equations presented in table 1 and the differential equations of table 2 are modified to become those presented in tables C-1 and C-2, below. The one-temperature model is unaffected by these modifications, since the streaming radiation is assumed to have been fully absorbed before the one-temperature model becomes applicable.

TABLE C-1

Divergent Three-Temperature Model Balance Equations

$$A = 4\pi R^2 \qquad V = \frac{4}{3}\pi R^3 = A R / 3 \tag{C-5}$$

$$E_s' V' = E_s V + Y f(t)\, dt - dE_{sm} V_{ave} - c\,(E_s/3)\, A\, dt + (E_s/3)\, dV \tag{C-6}$$

$$E_m' V' = E_m V + V_{ave}\,(dE_{sm} - dE_{mt}) + E_m\, dV \tag{C-7}$$

If $dR/dt > c/4$ then

$$E_t' V' = E_t V + dE_{mt} V_{ave} \tag{C-8}$$

and

$$c\,(E_s/3)\, A\, dt = [(E_s/3) + E_m]\, dV \tag{C-9}$$

Otherwise

$$E_t' V' = E_t V + dE_{mt} V_{ave} - \frac{c}{4} E_t A\, dt + E_t\, dV \tag{C-10}$$

and

$$A\,[c\,(E_s/3) + \frac{c}{4} E_t]\, dt = [(E_s/3) + E_t + E_m]\, dV \tag{C-11}$$

Where:

$$dE_{mt} = C(T_m)\,[aT_m^4 - E_t]\, dt \tag{C-12}$$

and

If $T_m = T_b$ and $[aT_m^4 - E_t] < E_s$

Then $dE_{sm}/dt = C(T_m)\,[aT_m^4 - E_t]$

Otherwise $dE_{sm}/dt = C(T_m)\, E_s$ (C-13)

TABLE C-2

Divergent Three Temperature Model Differential Equations

$$A = 4\pi R^2 \qquad V = \frac{4}{3}\pi R^3 = A R / 3 \tag{C-14}$$

$$\frac{d}{dt}(E_s V) = V\, dE_{sm}/dt + (E_s/3)\frac{dV}{dt} + Y f(t) - c\,(E_s/3)\,A \tag{C-15}$$

$$\frac{d}{dt}(VE_m) = V\,[dE_{sm}/dt - dE_{mt}/dt] + E_m \frac{dV}{dt} \tag{C-16}$$

If $dR/dt > c/4$ then

$$\frac{d}{dt}(VE_t) = V\,C(T_m)\,[aT_m^4 - E_t] \tag{C-17}$$

and

$$\frac{dV}{dt} = A\,c\,(E_s/3) / [(E_s/3) + E_m] \tag{C-18}$$

Otherwise

$$\frac{d}{dt}(VE_t) = V\,C(T_m)\,[aT_m^4 - E_t] + E_t \frac{dV}{dt} - \frac{c}{4} E_t\, A \tag{C-19}$$

and

$$\frac{dV}{dt} = A\,c\,[(E_s/3) + E_t/4] / [(E_s/3) + E_t + E_m] \tag{C-20}$$

Where:

$$dE_{mt}/dt = C(T_m)\,[aT_m^4 - E_t] \tag{C-22}$$

and

If $T_m = T_b$ and $[aT_m^4 - E_t] < E_s$

Then $dE_{sm}/dt = C(T_m)\,[aT_m^4 - E_t]$

Otherwise $dE_{sm}/dt = C(T_m)\,E_s$ (C-23)

Computer Program Modifications

The computer program listed in appendix A was modified to include the effects of spherical divergence of the streaming radiation. The modifications to the program follow directly from the modifications to the balance equations described above. The altered program lines are listed below:

```
1210 DV = DVS * (E.S/3) / (E.S/3 + E.M)
1310 DV = (DVS * (E.S/3) + DVT * E.T)
                / (E.S/3 + E.T + E.M)
1440 E.S = E.S * (1 - ((DVS+2*DV)/3)/V.NXT)
                - DE.SM * DILUTED + DE.S.YIELD
```

The global energy balance (upon which Line 1440 is based) has been rearranged to improve numerical performance.

Results of the Divergent Model

Figure C-1 shows the material and thermal radiation temperatures predicted by the divergent model for a one kiloton yield with a 2 shake square pulse. Figure C-2 compares T_{eff} from figure C-1 with T_{eff} as predicted by the homogeneous model and the early time model for the same yield pulse. Figures C-3 and C-4 present this same information for the case of a four megaton yield with a 5.14493 shake square pulse.

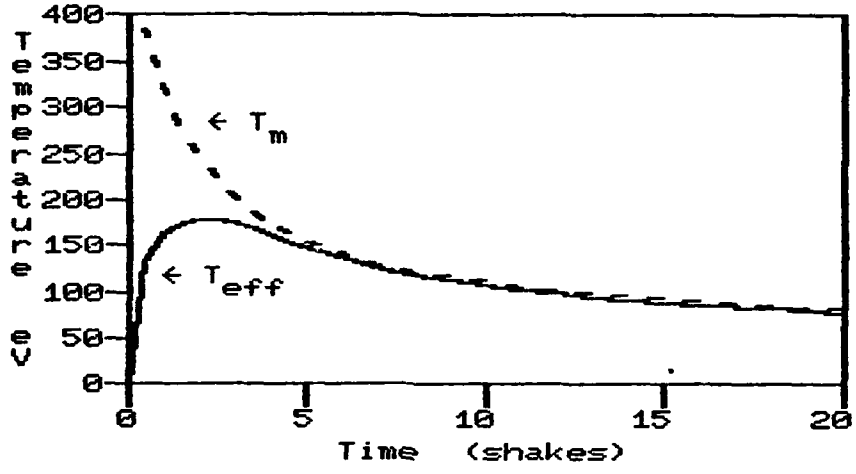

Fig. C-1 Divergent Model Temperatures

for One Kiloton Yield with 2 Shake Square Pulse

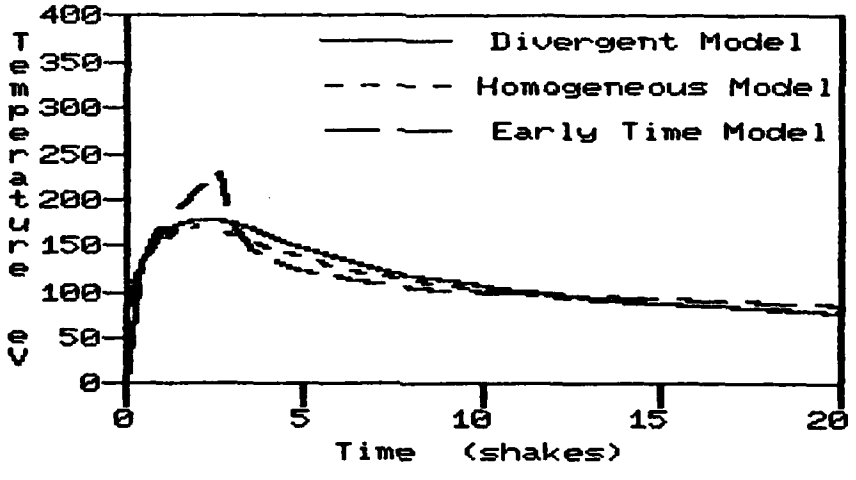

Fig. C-2 Effective Temperatures for the Three Models

for One Kiloton Yield with 2 Shake Square Pulse

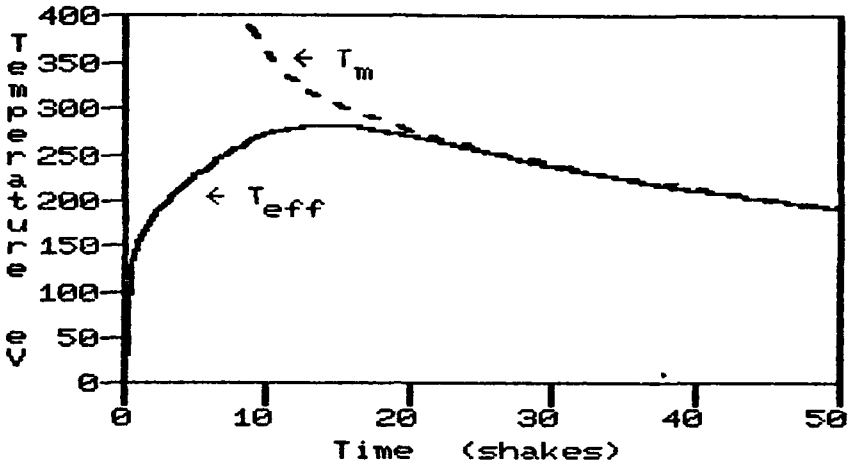

Fig. C-3 Divergent Model Temperatures

for Four Megaton Yield with 5.14493 Shake Square Pulse

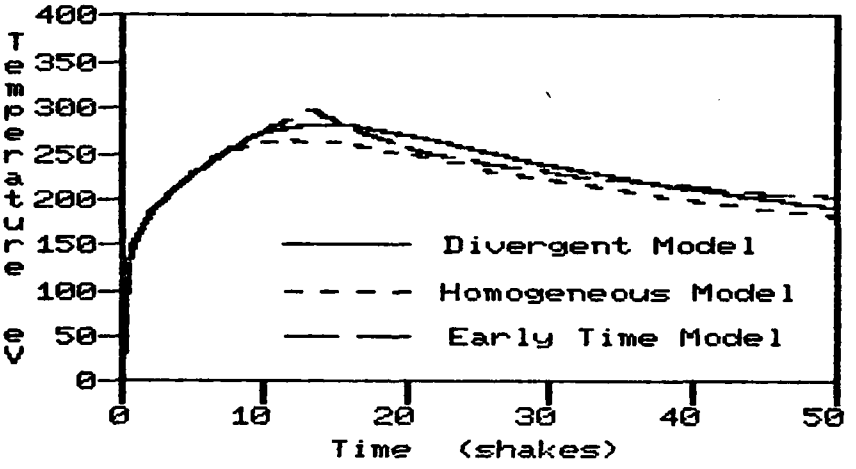

Fig. C-4 Effective Temperatures for the Three Models

for Four Megaton Yield with 5.14493 Shake Square Pulse

Figure C-5 compares the radius predicted by the divergent model with that predicted by the early time model and by the (unmodified) homogeneous model for the case of twenty kiloton yield with a 5.14493 shake square pulse. This is the case used for the examples in sections II and VI.

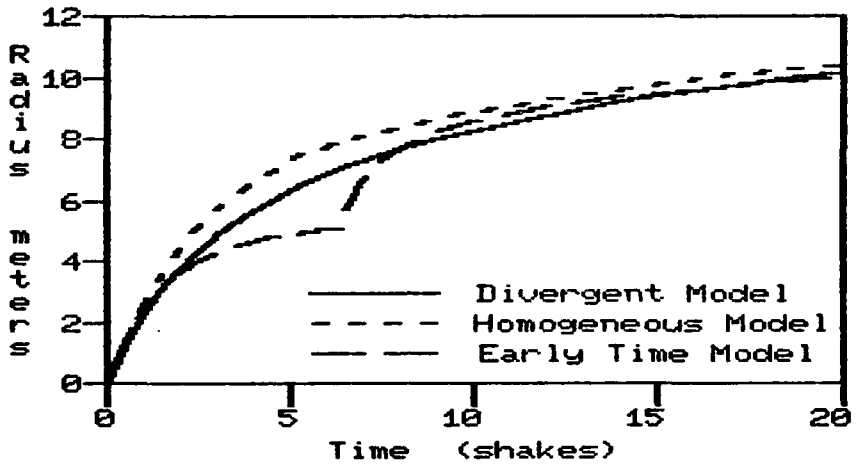

Fig. C-5 Radius for the Three Models
for Twenty Kiloton Yield with a 5.14493 Shake Square Pulse

Observations

The temperature curves predicted by the divergent model do not differ qualitatively from those of the (unmodified) homogeneous model. The addition of spherical divergence does result in a somewhat improved agreement with the early time model, but the use of a state-of-the-art computer code to determine the "right" answer would be

needed to choose between the two versions of the homogeneous model.

At first thought, it might seem that reducing the streaming radiation by a factor of three would decrease the growth rate by a factor of about three, but figure C-5 shows this not to be the case. There are several reasons for this insensitivity:

— If E_s is quite large compared to E_m, then even $E_s/3$ is large compared to E_m, and dR/dt is near the speed of light and is insensitive to E_s.

— If E_t is large compared to E_s, then E_t determines dR/dt, rather than E_s.

— If dR/dt is decreased somewhat (which it is), then the volume will be smaller (by the ratio of radii cubed) and the radiation energy will have a higher average density, which tends to offset the effect of the 1/3 factor in $E_s(R)$, and prevent dR/dt from decreasing as much as anticipated.

In any event, the divergent model provides very good agreement (in predicting the radius) with the early time model during the early part of the yield pulse for a square pulse. This is as expected, for during this period, absorption is small compared with divergence, and the streaming radiation yield history is constant.

Conclusions

1. The inclusion of spherical divergence of the streaming radiation provides some improvement in agreement with the early time model with respect to temperatures, and more improvement with respect to radius.

2. The improvement is quantitative and small, rather than qualitative. It is doubtful whether the additional complications are justified by the improvement if the homogeneous model is used pedagogically. Some students may object to the assumption of uniform streaming energy density in the homogeneous model. The modifications developed in this appendix could be of value as a response to such objections.

3. The homogeneous model has been shown to be very insensitive to large variations in the assumed distribution of the streaming radiation. This tends to explain the reasonably good numerical results obtained by the model, and is the most important conclusion of this appendix. The assumption of spatially uniform E_s may be a poor assumption in and of itself, but the model is so insensitive to the distribution, whatever it may be, that the assumption is adequate for the purpose.

Appendix D

Method for Recursive Evaluation of the Integrals in the Early Time Model Integro-Differential Equations

Statement of the Problem

Pomraning's early time model [Ref 2] consists of a linked system of integro-differential equations, for the burnout phase. In reference 3, Pomraning presents a finite differencing scheme for integrating this system. This scheme requires a trapezoidal integration of each of two integrals (which are coefficients in the differential equations) at each time step. This approach, although straight-forward, requires maintaining arrays of values of the variables in the integrands, amounting to thousands of floating point numbers, as well as causing expense in execution time. These drawbacks would have precluded implementation of the model on the personal microcomputer used for this research. It was therefore necessary to derive a recursive system for evaluation of these integrals. This appendix presents the recursive method which was used.

Integrals to be Evaluated

The integrals to be evaluated appear in equations (41) and (42) of reference 2 (equations (42) and (43) of reference 3). Using γ as the dummy of integration, rather than Pomraning's t', the integrals to be evaluated are:

$$I(t) = \int_0^R [V(\tau)/V(t)]\, e^{-b(t-\tau)}\, d\tau \qquad \text{(D-1)}$$

and

$$H(t) = \int_0^R r^2\, S\left(t - \frac{R-r}{c}\right) dr \,/\, c^3 \qquad \text{(D-2)}$$

where

$$b = \rho c\, K(T_b) \qquad \text{(D-3)}$$

and

$$S(t) = b\,[aT_b^4 - E_t(t)] \qquad \text{(D-4)}$$

Recursion Relation for I(t)

Let I_i indicate $I(t_i)$, where t_i is the i'th time in a finite differencing scheme, and assume that I_i (and the other variables at time t_i) are known, as is V_{i+1}. The objective is to find a formula for I_{i+1} in terms of I_i and V_{i+1}. Let the time increment be δt, then

$$\delta t = t_{i+1} - t_i \qquad \text{(D-5)}$$

Using this notation, equation (D-1) evaluated at $t+\delta t$ becomes:

$$I_{i+1} = \int_0^{t+\delta t} [V(\tau)/V_{i+1}]\; e^{-b(t+\delta t-\tau)}\, d\tau \qquad \text{(D-6)}$$

Segmenting the interval of integration and rearranging:

$$I_{i+1} = [V_i/V_{i+1}] \int_0^t [V(\tau)/V_i]\ e^{-b(t-\tau)}\ e^{-b\cdot\delta t}\ d\tau$$

$$+ \int_t^{t+\delta t} [V(\tau)/V_{i+1}]\ e^{-b(t-\tau+\delta t)}\ d\tau \qquad \text{(D-7)}$$

The first integral in equation (D-7) is proportional to I_i and the second can be evaluated using the trapezoidal rule:

$$I_{i+1} = (V_i/V_{i+1})\ e^{-b\cdot\delta t}\ I_i + [1 + (V_i/V_{i+1})\ e^{-b\cdot\delta t}]\ \delta t / 2 \qquad \text{(D-8)}$$

For computational efficiency, using a constant time increment δt, let

$$\eta = (V_i/V_{i+1})\ e^{-b\cdot\delta t} \qquad \text{(D-9)}$$

and

$$C_i = \rho\, c\, K\, a\, T_b^4 \qquad \text{(D-10)}$$

Then $E_t(t) = C_i\ I(t)$, and Pomraning's equation (41) becomes the desired recursion relation:

$$E_{i+1} = \eta\, E_i + C_i\ t\ (1 + \eta)\ /\ 2 \qquad \text{(D-11)}$$

where E_i indicates $E_t(t_i)$.

This is the basis for line 1050 of the program listed in Appendix E.

Conversion to Retarded Time Integration for H(t)

It is convenient to maintain a list, S_i, of $S(t_i)$, but awkward to convert these values to correspond to steps of dr for S(t-(R-r)/c). Thus, it is efficient to change variables from r to τ, where τ is defined by

$$r = c\,(\tau - t') \qquad \text{(D-12)}$$

where

$$t' = t - R(t)/c \qquad \text{(D-13)}$$

The physical significance of t' is that t' is the time of emission of the streaming radiation which reaches the surface of the fireball, R(t), at time t. Similarly, τ is the time of emission of the streaming radiation which reaches radius r at time t. Thus, these are retarded times in the sense of the retarded potentials of electromagnetic theory.

The transformed integral for H(t) is:

$$H(t) = \int_{t'}^{t} (\tau - t')^2 \; S(\tau) \; d\tau \qquad \text{(D-14)}$$

Approach for H(t)

The related integral forms, F(t) and G(t), will be needed for the recursion relation for H(t). These are defined by:

$$F(t) = \int_{t'}^{t} S(\tau)\ d\tau \qquad \text{(D-15)}$$

$$G(t) = \int_{t'}^{t} (\tau - t')\ S(\tau)\ d\tau \qquad \text{(D-16)}$$

It may be noted that these forms are similar to Volterra integrals with difference kernels. However, t' is an implicit function of t, which complicates use of Leibnitz' rule such that no useful simplifications could be found in that direction.

Techniques similar to those used for I(t), above, lead to a recursion relation for H_{i+1} in terms of H_i, G_i, and other known quantities. A recursion relation is then needed for G_{i+1}, and is found to be in terms of G_i, F_i, etc. The recursion relation then needed for F_{i+1} is only in terms of F_i and known quantities, completing the recursive system. To simplify the presentation, the recursion relations are derived in increasing order of complexity, from F to H.

Recursion Relation for F(t)

Segmenting the interval of integration of equation (D-15), and evaluating at t_{i+1} for F_{i+1}:

$$F_{i+1} = F_i + \int_{t_i}^{t_{i+1}} S(\tau)\ d\tau - \int_{t_i'}^{t_{i+1}'} S(\tau)\ d\tau \qquad \text{(D-17)}$$

The integrals in equation (D-17) are evaluated using the trapezoidal rule, which produces the desired recursion relation:

$$F_{i+1} = F_i + \delta t\ (S_{i+1} + S_i)\ /\ 2 - \delta t'\ (S'_{i+1} + S'_i)\ /\ 2 \qquad \text{(D-18)}$$

where

$$S'_i = S(t'_i) \qquad \text{(D-19)}$$

$$\delta t' = t'_{i+1} - t'_i = \delta t - \delta R/c \qquad \text{(D-20)}$$

$$\delta R = R_{i+1} - R_i \qquad \text{(D-21)}$$

and where $S'_{i+1} = S(t'_{i+1})$ is obtained by linear interpolation in the list of S_i. (Note that $t'_{i+1} < t_{i+1}$ so it is always possible to perform the interpolation.) S'_{i+1} is retained for use as S'_i at the next time step, so only one (interpolated) table look-up is required at each time step.

Recursion Relation for G(t)

Development of the recursion relation for G_{i+1} will be simplified by the following notation: define G(a,b) by

$$G(a,b) = \int_a^b (\tau - t' - \delta t')\ S(\tau)\ d\tau \qquad \text{(D-22)}$$

Then, $G_{i+1} = G(t'_{i+1}, t'_i) = G(t'+\delta t', t+\delta t)$ where the subscript "i" is dropped. Using this notation and segmenting

the interval of integration as before:

$$G_{i+1} = G(t',t) + G(t,t+\delta t) - G(t',t'+\delta t') \qquad \text{(D-23)}$$

The three terms on the right of this equation will now be evaluated. Note that $G(t',t) \neq G_i$ because of the $-\delta t'$ in the integrand of equation (D-22). Since $\delta t'$ is a constant with respect to the integration, however, the integration can be simplified as follows:

$$G(t',t) = \int_{t'}^{t} (\tau - t')\, S(\tau)\, d\tau - \delta t' \int_{t'}^{t} S(\tau)\, d\tau \qquad \text{(D-24)}$$

Recalling equations (D-15) and (D-16):

$$G(t',t) = G_i - \delta t'\, F_i \qquad \text{(D-25)}$$

The second term in (D-23) is evaluated by the trapezoidal rule as:

$$G(t,t+\delta t) = \delta t\, [(t+\delta t-t'-\delta t')\, S_{i+1} + (t-t'-\delta t')\, S_i] / 2 \qquad \text{(D-26)}$$

This is simplified by substituting the definition of the retarded time, $t'_{i+1} = t_{i+1} - R_{i+1}/c$ so that

$$t+\delta t-t'-\delta t' = t_{i+1} - t'_{i+1} = R_{i+1}/c \qquad \text{(D-27)}$$

which leads to

$$t-t'-\delta t' \approx R_{i+1}/c - \delta t \qquad \text{(D-28)}$$

Substituting equations (D-27) and (D-28) into (D-26) gives

$$G(t,t+\delta t) = \delta t \left[S_{i+1} R_{i+1}/c + S_i (R_{i+1}/c - \delta t)\right] / 2 \qquad \text{(D-29)}$$

The third term in equation (D-23) is evaluated similarly as:

$$G(t',t'+\delta t') = \delta t' \left[(t'+\delta t'-t'-\delta t') S'_{i+1} + (t'-t'-\delta t') S'_i\right] / 2 \qquad \text{(D-30)}$$

which simplifies algebraically to

$$G(t',t'+\delta t') = - \delta t'^2 S'_i / 2 \qquad \text{(D-31)}$$

Substituting equations (D-25), (D-29) and (D-31) into (D-23) gives the desired recursion relation for G(t):

$$G_{i+1} = G_i - \delta t' F_i + \delta t'^2 S'_i / 2 + \delta t \left[S_{i+1} R_{i+1}/c + S_i (R_{i+1}/c - \delta t)\right] / 2 \qquad \text{(D-32)}$$

This recursion relation is entirely in terms of known quantities and requires no additional table look-ups.

Recursion Relation for H(t)

The approach for H(t) is the same as that for G(t). Let H(a,b) be defined by:

$$H(a,b) = \int_a^b (\tau - t' - \delta t')^2 \; S(\tau) \; d\tau \qquad \text{(D-33)}$$

Then equation (D-14) evaluated at t_{i+1} becomes

$$H_{i+1} = H(t',t) + H(t,t+\delta t) - H(t',t'+\delta t') \qquad \text{(D-34)}$$

The integral for H(t',t) is evaluated by expanding the square in the integrand and expressing the result as the sum of three integrals, as follows:

$$H(t',t) = \int_{t'}^{t} (\tau - t')^2 \; S(\tau) \; d\tau$$

$$- 2 \, \delta t' \int_{t'}^{t} (\tau - t') \; S(\tau) \; d\tau$$

$$+ \delta t'^2 \int_{t'}^{t} S(\tau) \; d\tau \qquad \text{(D-35)}$$

These expressions are the reason for the original choice of the definitions of F(t) and G(t). Substitution of those definitions gives

$$H(t',t) = H_i - 2 \, \delta t' \, G_i + \delta t'^2 \, F_i \qquad \text{(D-36)}$$

The second term in equation (D-34) is evaluated using the trapezoidal rule to obtain:

$$H(t,t+\delta t) = \delta t \left[(t+\delta t-t'-\delta t')^2 S_{i+1} + (t-t'-\delta t')^2 S_i\right] / 2 \qquad \text{(D-37)}$$

Substituting equations (D-27) and (D-28) gives the computationally convenient form:

$$H(t,t+\delta t) = \delta t \left[(R_{i+1}/c)^2 S_{i+1} + (R_{i+1}/c - \delta t)^2 S_i\right] / 2 \qquad \text{(D-38)}$$

The third term in equation (D-34) is evaluated using the trapezoidal rule to obtain:

$$H(t',t'+\delta t') = \delta t' \left[(t'+\delta t'-t'-\delta t')^2 S'_{i+1} + (t'-t'-\delta t')^2 S'_i\right] / 2 \qquad \text{(D-39)}$$

which simplifies algebraically to:

$$H(t',t'+\delta t') = \delta t'^3 S'_i / 2 \qquad \text{(D-40)}$$

Substituting equations (D-36), (D-38) and (D-40) in equation (D-34) produces the desired recursion relation for H(t):

$$H_{i+1} = H_i - 2\,\delta t' G_i + \delta t'^2 F_i - \delta t'^3 S'_i / 2 + \delta t \left[(R_{i+1}/c)^2 S_{i+1} + (R_{i+1}/c - \delta t)^2 S_i\right] / 2 \qquad \text{(D-41)}$$

TABLE D-1

Recursive System for Evaluation of the Retarded Time Integral, H(t)

$$F_{i+1} = F_i + \delta t\,(S_{i+1} + S_i)/2 - \delta t'\,(S'_{i+1} + S'_i)/2 \qquad \text{(D-18)}$$

$$G_{i+1} = G_i - \delta t'\,F_i + \delta t'^2\,S'_i/2 + \delta t\,[S_{i+1}\,R_{i+1}/c + S_i\,(R_{i+1}/c - \delta t)]/2 \qquad \text{(D-32)}$$

$$H_{i+1} = H_i - 2\,\delta t'\,G_i + \delta t'^2\,F_i - \delta t'^3\,S'_i/2 + \delta t\,[(R_{i+1}/c)^2\,S_{i+1} + (R_{i+1}/c - \delta t)^2\,S_i]/2 \qquad \text{(D-41)}$$

where:

$$t' = t - R(t)/c \qquad \text{(D-13)}$$

$$S'_i = S(t'_i) \qquad \text{(D-19)}$$

$$\delta t' = t'_{i+1} - t'_i = \delta t - \delta R/c \qquad \text{(D-20)}$$

$$\delta R = R_{i+1} - R_i \qquad \text{(D-21)}$$

and where $S'_{i+1} = S(t'_{i+1})$ is obtained by linear interpolation in the list of S_i.

Conclusions

The recursive system for evaluation of H(t) is summarized in Table D-1. The system has the advantages of being entirely algebraic and of requiring only one (interpolated) table look-up at each time step. If a constant time increment, δt, is used, the table look-up becomes an algebraic calculation, rather than a search. These features speed program execution significantly (from 80 hours using the trapezoidal integrations, estimated based on the execution time of the example case described below, to 12 minutes using the recursion relations). They also minimize computer storage space requirements, since only a list of S values need be maintained. This recursive system is the basis of lines 1140 through 1230 of the program listed in Appendix E.

Benchmark Comparison

The numerical accuracy of this method was verified by comparison with computation directly by trapezoidal rule. The example case used was evaluation at a single time step at the end of the burnout phase for a four megaton burst. The results of the two calculations agreed identically (to the limit of precision carried). To verify the entire implementation of Pomraning's model, a more complex program, of which the program listed in Appendix E is a subset, was used. This larger program included the effects of the

ground. The example chosen (4 MT burst at 1 m height, exponential pulse shape with $\alpha = \beta = 0.6$ shake^{-1}) duplicated that used in reference 2. This example case served as a benchmark. The results, $T_m(t)$ and $T_{eff}(t)$, obtained with this program matched those graphed in reference 2, within the precision with which that graph could be read. This agreement was obtained for the burnout and diffusion phases, verifying the validity of both programs.

Appendix E

Basic Computer Program

for

Burnout Phase of the Early Time Model

This version of the program assumes a triangular yield pulse of isosceles shape. It is a more-or-less straightforward implementation of Pomraning's finite differencing scheme [Ref 3]. An important exception is that the explicit computation of integrals as coefficients at each time step has been replaced by recursive schemes, as derived in appendix D. Variable names follow the notation of reference 3 and appendix D, above. "RET" in variable names stands for "retarded", thus T.RET is t'_i, T.RET.NXT is t'_{i+1}

```
50 WIDTH LPRINT 80
110 DEFINT I-N
120 DIM S(4000)
150 DATA 3.1315E10, 8.9217E-2, 1.86988E12, 3.50998E11, 3,
        4.18879, 339.292, 4.96E10, 3.14159, .519739
160 READ C1, C2, CQ, CE, CL, C4PI3, C4PC3, Q, PI, CT
170 HOME
    : VTAB 2
180 PRINT "Enter parameters for triangular yield function:"
```

```
     : PRINT
190 HTAB 10
     : INPUT  "Pulse Width (shakes):  T.pulse  = ",T.PULSE
200 T.PK = T.PULSE / 2
220 PRINT
240 PRINT
     : PRINT "Enter Burst Parameters:"
     : PRINT
250 HTAB 10
     : INPUT "Yield (kiloton) = ", YIELD
     : YIELD = YIELD * 4.2E+12  'Convert kilotons to Joules
270 YDOT.PK = YIELD / T.PK
280 PRINT
     : PRINT "Enter Quadrature Parameters:"
     : PRINT
290 HTAB 10
     : INPUT "Time Increment (shakes) = ", DELTA.T#
     : DT = DELTA.T#
300 PRINT
     : C.DECAY = EXP(-C2*DT)
310 HTAB 10
     : INPUT "Number of steps per printout = ", N.PRINT
320 PRINT
     : PRINT "Commencing computations"
330 GOTO 500
```

```
350 'Data Lprint Subroutine
360 LPRINT T, T.RET, R, V, Y.INTEG
365 T.EFF = CT * SQR(SQR(E))
370 LPRINT T.EFF,E,S,U,R.DOT
380 LPRINT F,G,H
390 LPRINT
400 RETURN

500 'Initialization of variables
510 R.DOT = CL
520 R=0
530 V=0
550 S=C1
560 S(0)=S
580 E=0
590 I=0
600 T=0
610 T.RET=0
620 IF DT > T.PK
      THEN PRINT "Error: pulse shorter than increment!!"
           : BEEP 25,100:STOP
      ELSE U = YDOT.PK * DT / 2 / T.PK
630 F=0
640 G=0
650 H=0
```

```
660 Y.INTEG=0

700 'Initial printout
710 LPRINT "Burnout Phase Fireball Growth Program:"
711 LPRINT
"Version 2.1tr  --  Single Precision, No Ground Effects"
     : LPRINT "Yield (KT) = ";YIELD/4.2E+12
712 LPRINT
     : LPRINT "Pulse Shape Parameters:"
713 LPRINT "   Triangular Pulse:"
     : LPRINT "    start at t = 0,  peak at t =";T.PK;
              " stop at t =";T.PULSE
714 LPRINT "   Peak Yield Rate (J/shake) =";YDOT.PK
715 LPRINT
716 LPRINT "Quadrature Parameters:"
717 LPRINT "   Time Increment (shake) = ";DT
718 LPRINT "   Number per printout    = ";N.PRINT
719 LPRINT: LPRINT: LPRINT
720 LPRINT "T (shake)","T.retarded","Radius (m)",
             "V (m^3)","Y.integ (J)"
730 LPRINT "T.eff (eV)","E-th (J/m^3)","S (J/m^3/sh)",
                   "U (J/shake)","dR/dt (m/sh)"
740 LPRINT "F (J/m^3)","G (J-sh/m^3)","H (J-sh^2/m^3)"
750 LPRINT
760 GOSUB 350 'data lprint
```

```
1000 'Main Iteration Routine
1010 R.NXT = R + R.DOT * DT
1020 V.NXT = C4PI3 * R.NXT * R.NXT * R.NXT
1040 ETA = (V / V.NXT) * C.DECAY
1050 E.NXT = ETA * E + C1 * DT * (1 + ETA) / 2
1060 T.NXT = (I+1) * DELTA.T#
1070 T.RET.NXT = T.NXT - R.NXT/CL
1080 DT.RET = T.RET.NXT - T.RET
1090 S.NXT = C2 * (CE - E.NXT)
1100 S(I+1) = S.NXT
1110 I.RET.NXT = FIX(T.RET.NXT / DT)
1120 S.RET.NXT = S(I.RET.NXT)
          + (T.RET.NXT / DT - I.RET.NXT)
               * (S(I.RET.NXT+1) - S(I.RET.NXT))

1140 'Recursive system to eval integrals of S(t)
1150 A1 = DT * S / 2
1160 A2 = DT * S.NXT / 2
1170 A3 = DT.RET * S.RET / 2
1180 A4 = DT.RET * S.RET.NXT / 2
1190 F.NXT = F + A1 + A2 - A3 - A4
1200 A6 = R.NXT / CL
1210 A5 = A6 - DT
1220 G.NXT = G - DT.RET * (F-A3) + A1 * A5 + A2 * A6
1230 H.NXT = H + DT.RET * (-2*G + DT.RET * (F-2*A3/3))
               + A1*A5*A5 + A2*A6*A6
```

```
1232 IF T.RET.NXT = 0
       THEN YDOT.RET.NXT = U
            : GOTO 1240 'Note: the GOTO is part of the THEN
1235 IF T.RET.NXT >= T.PULSE
          THEN YDOT.RET.NXT = 0
     ELSE IF T.RET.NXT <= T.PK
          THEN YDOT.RET.NXT = YDOT.PK * T.RET.NXT / T.PK
     ELSE YDOT.RET.NXT = YDOT.PK
                              * (T.PULSE-T.RET.NXT) / T.PK
1240 U.NXT = YDOT.RET.NXT - C4PC3 * CSNG(H.NXT)
1250 R.DOT = CL / (1 + CQ * R.NXT * R.NXT / U.NXT)
1260 R=R.NXT
1270 V=V.NXT
1290 E=E.NXT
1300 T=T.NXT
1310 T.RET=T.RET.NXT
1320 S=S.NXT
1330 S.RET=S.RET.NXT
1350 F=F.NXT
1360 G=G.NXT
1370 H=H.NXT
1380 U=U.NXT
1390 I=I+1
```

```
1400 'End-of-Phase Criteria checks
1410 IF T>T.PULSE
          THEN Y.INTEG = YIELD
     ELSE IF T<=T.PK
          THEN Y.INTEG = YDOT.PK * T * T / 2 / T.PK
     ELSE Y.INTEG = YIELD
           - YDOT.PK * (T.PULSE-T) * (T.PULSE-T) / 2 / T.PK
1430 IF U<=0 OR V*(Q+E)>=Y.INTEG
       THEN GOSUB 350: GOTO 2000

1500 'Printout Criteria Check
1510 IF (I MOD N.PRINT) = 0
       THEN GOSUB 350

1600 'Loop to next iteration
1610 GOTO 1000

2000 'Problem completed,
          Loop back to input routine for next problem
2010 LPRINT CHR$(12) 'Form Feed
2020 BEEP 40, 250
     : GOTO 170
 'Beep sounds speaker to notify operator ready for next case
2030 END  'Not Executed, present for compiler only
```

Notes at end of Appendix A are applicable to this program.

Appendix F

Basic Computer Program

for

Diffusion Phase of the Early Time Model

This version of the program assumes a triangular yield pulse of isosceles shape. It assumes that the end of the burnout phase occurs after the peak of the yield pulse but before the end of the pulse. If the end of the burnout phase is in fact after the end of the yield pulse for a particular problem, a revised version of the program (which eliminates the terms for yield rate contribution to E_s) should be used. This program implements Pomraning's finite differencing scheme [Ref 3].

```
50 WIDTH LPRINT 80
60 DEFINT I-N
70 DEF FNCOEF(T) = RHO.KAPPA.C
                   * (T.B/T.M) * (T.B/T.M) * (T.B/T.M)
75 DEF FNG(T) = GO * (T/T.B) * (T/T.B) * (T/T.B)
90 DATA 8.9217E-2, 13.7, 400, 3, 3.14159, 4.96E10,
        1.24E8, 296.973
100 READ RHO.KAPPA.C, A, T.B, C, PI, E.B, C.V, GO
110 HOME
    : VTAB 2
120 PRINT "Enter parameters for triangular yield function:"
```

```
     : PRINT
160 PRINT
     : PRINT "Enter Burst Parameters:"
     : PRINT
170 HTAB 10
     : INPUT "Pulse Width (shakes):  T.PULSE = ",T.PULSE
180 T.PK = T.PULSE / 2
190 HTAB 10
     : INPUT "Yield (kiloton) = ", YIELD
     : YIELD = YIELD * 4.2E+12 'Convert kilotons to Joules
195 YDOT.PK = YIELD / T.PK
200 PRINT
     : PRINT "Enter Quadrature Parameters:"
     : PRINT
210 HTAB 10
     : INPUT "Time Increment (shakes) = ", DELTA.T#
     : DT = DELTA.T#
220 PRINT
230 HTAB 10
     : INPUT "Number of steps per printout = ", N.PRINT
240 PRINT
     : HTAB 10
     : INPUT "Initial Time: ",T#
     : T = T#
242 PRINT
```

```
     : HTAB 10
     : INPUT "Initial Counter: ",I
244 PRINT
     : HTAB 10
     : INPUT "Maximum time to which to compute: ",T.QUIT
250 PRINT
     : HTAB 10
     : INPUT "Yield delivered so far: ",YSUM
260 PRINT
     : HTAB 10
     : INPUT "Initial thermal energy density
     :  E.T = ",E.T
265 PRINT
     : HTAB 10
     : INPUT "Initial material energy density
               (0 for default):  E.M = ",E.M
270 PRINT
     : HTAB 10
     : INPUT "Initial Volume:  V = ",V
280 GOTO 400

300 'Data Lprint Subroutine
310 LPRINT T, V, R, R.DOT
320 T.EFF = SQR (SQR (E.T / A) )
330 LPRINT E.S, E.M, E.T, T.M, T.EFF
```

```
340 LPRINT
350 RETURN

400 'Initialization of variables
410 IF E.M = 0
       THEN E.M = 4.96E+10
420 E.S = YSUM / V - E.M - E.T
430 T.M = E.M / C.V
440 R = (.75*V/PI)^(1/3)
450 R.DOT = 0
460 IF T > T.PULSE
          THEN PRINT "Error: use version
                        'DB01PT1' if pulse is already over"
               : BEEP 25,200
               : STOP
     ELSE IF T<T.PK
          THEN PRINT "Error: initial time < t.peak
                          not supported"
               : BEEP 25,200
               : STOP
465 YSUM = YIELD
           - YDOT.PK * (T.PULSE-T) * (T.PULSE-T) / 2 / T.PK
470 Q.M = E.M * V
480 Q.S = E.S * V
490 Q.T = E.T * V
```

```
600 'Initial printout
610 LPRINT "Diffusion Phase Radiative Fireball Growth
              Program based on Pomraning's model:"
620 LPRINT "Version 1.2 -- Single Precision
         -- Radii assume spherical fireball"
     : LPRINT "--  Triangular pulse yield integration"
     : LPRINT "YIELD (KT) = ";YIELD/4.2E+12
630 LPRINT
     : LPRINT "Pulse Shape Parameters:"
640 LPRINT "   Triangular Pulse:"
650 LPRINT "     start at t = 0   peak at t =";T.PK;
            "  stop at t =";T.PULSE
660 LPRINT
670 LPRINT "Quadrature Parameters:"
680 LPRINT "   Time Increment (shake) = ";DT
690 LPRINT "   Number per printout    = ";N.PRINT
700 LPRINT: LPRINT: LPRINT
710 LPRINT "T (shake)","V (m^3)","Radius (m)",
           "dR/dt (m/shake)"
720 LPRINT "E.s (J/m^3)","E.m (J/m^3)","E.th (J/m^3)",
           "T.m (eV)","T.eff (eV)"
730 LPRINT
740 GOSUB 300 'data lprint
```

```
1000 'Main Iteration Routine
1010 'Compute coefficients
1020 IF T.M = T.B
        THEN RHO.KAPPA.C.OF.T = RHO.KAPPA.C
           : G = GO
        ELSE RHO.KAPPA.C.OF.T = FNCOEF(T.M)
           : G = FNG(T.M)
1030 AO = RHO.KAPPA.C.OF.T
1040 IF T+DT > T.PULSE
        THEN YSUM.NXT = YIELD
        ELSE YSUM.NXT = YIELD
                          - YDOT.PK * (T.PULSE-T-DT)
                              * (T.PULSE-T-DT) / 2 / T.PK
1050 DY = YSUM.NXT-YSUM
1060 YSUM = YSUM.NXT
1070 EPS = (G*Q.T*DT/V^(2/3) - DY) / YSUM
1080 IF EPS < .001
        THEN V.NXT = V * (1 + 3 * EPS)
        ELSE V.NXT = V * (1 + EPS) * (1 + EPS) * (1 + EPS)
1090 A1 = 1 + AO * DT
1100 A2 = A * T.M * T.M * T.M / C.V

1200 'Compute new energy partition among
                 streaming, material, thermal radiation
1210 Q.S.NXT = (Q.S + DY) / A1
1220 A3 = 1 + AO * DT * (1 + A2)
```

```
1230 Q.M.NXT = (Q.M * A1 + Q.S.NXT * A0 * DT * A1
                                    + Q.T * A0 * DT) / A3
1240 Q.T.NXT = (Q.T + A0 * A2 * Q.M.NXT * DT) / A1

1300 'Set variables to next values
1310 Q.M = Q.M.NXT
1320 Q.T = Q.T.NXT
1330 Q.S = Q.S.NXT
1340 E.M = Q.M / V
1350 E.T = Q.T / V
1360 E.S = Q.S / V
1370 T.M = E.M / C.V
1390 V = V.NXT
1400 R.NXT = (.75 * V / PI) ^ (1/3)
1410 R.DOT = (R.NXT - R) / DT
1420 R = R.NXT
1430 T# = T# + DELTA.T#
1440 T = T#
1450 I = I + 1

1500 'End-of-Phase Criteria checks
1510 IF T.M <= 25 OR T>=T.QUIT
       THEN GOSUB 300
          : GOTO 1600  'Note: GOTO is part of THEN
```

```
1520 'Printout Criteria Check
1530 IF (I MOD N.PRINT) = 0
       THEN I = 0
          : GOSUB 300
1540 'Loop to next iteration
1550 GOTO 1000

1600 'End of Radiative only fireball growth.
     Hydroseparation assumed to occur at temp of 25 eV
     or T.quit was reached first
1610 LPRINT CHR$(12) 'Form Feed
1615 BEEP 40,250
     : GOTO 110  'Loop back to input routine for next case
1620 END  'Not executed, present for compiler only
```

Notes at end of Appendix A are applicable to this program.

Vita

PII Redacted

Kirk Alan Mathews [redacted] He graduated from high school in Federal Way, Washington in 1967 and attended the California Institute of Technology, Pasadena, California, from which he received the degree of Bachelor of Science with majors in Physics and English Literature, in June 1971. He attended the University of Washington, Graduate School of Nuclear Engineering until called to active duty at the Naval Officer Candidate School in January 1972. He received his regular commission as a Distinguished Naval Graduate on 12 May 1972. He graduated at the head of his class at the Naval Nuclear Power School, Mare Island, California, in November 1972, and completed Nuclear Prototype training at the D1G prototype, at West Milton, New York, in May 1973. He qualified in submarines while serving in USS George Washington, SSBN 598, until November 1975. He then taught nuclear reactor dynamics and core characteristics to officer students at the Nuclear Power Schools at Mare Island, Calif., and Orlando, Florida, qualifying as a nuclear propulsion plant Engineer Officer during this period. He reported aboard USS Birmingham, SSN 695, at her launching in November 1977, as Navigator and Operations Officer. He was a shift senior supervisor for the nuclear propulsion plant construction and testing of USS Birmingham, which was commissioned 16 December 1978. He entered the School of Engineering, Air Force Institute of Technology, in June 1981. He is a member of Tau Beta Pi.

UNCLASSIFIED

SECURITY CLASSIFICATION OF THIS PAGE (When Data Entered)

REPORT DOCUMENTATION PAGE	READ INSTRUCTIONS BEFORE COMPLETING FORM
1. REPORT NUMBER: AFIT/GNE/PH/83M-9	2. GOVT ACCESSION NO.: AD-A124793
3. RECIPIENT'S CATALOG NUMBER:	
4. TITLE (and Subtitle): THREE - TEMPERATURE HOMOGENEOUS MODEL OF THE RADIATIVE GROWTH PHASE OF A FREE AIR NUCLEAR FIREBALL	5. TYPE OF REPORT & PERIOD COVERED: MS THESIS
	6. PERFORMING ORG. REPORT NUMBER:
7. AUTHOR(s): KIRK A. MATHEWS, LCDR USN	8. CONTRACT OR GRANT NUMBER(s):
9. PERFORMING ORGANIZATION NAME AND ADDRESS:	10. PROGRAM ELEMENT, PROJECT, TASK AREA & WORK UNIT NUMBERS:
11. CONTROLLING OFFICE NAME AND ADDRESS: AIR FORCE INSTITUTE OF TECHNOLOGY (AFIT/EN) WRIGHT-PATTERSON AFB OHIO 45433	12. REPORT DATE: DECEMBER 1982
	13. NUMBER OF PAGES: 141
14. MONITORING AGENCY NAME & ADDRESS(if different from Controlling Office):	15. SECURITY CLASS. (of this report): UNCLASSIFIED
	15a. DECLASSIFICATION/DOWNGRADING SCHEDULE:

16. DISTRIBUTION STATEMENT (of this Report)

APPROVED FOR PUBLIC RELEASE; DISTRIBUTION UNLIMITED.

17. DISTRIBUTION STATEMENT (of the abstract entered in Block 20, if different from Report)

APPROVED FOR PUBLIC RELEASE; DISTRIBUTION UNLIMITED.

Fredrick Lynch, Major, USAF
Director of Public Affairs

18. SUPPLEMENTARY NOTES

Approved for public release: IAW AFR 190-17.

LYNN E. WOLAVER
Dean for Research and Professional Development
Air Force Institute of Technology (AIC)
Wright-Patterson AFB OH 45433

4 JAN 1983

19. KEY WORDS (Continue on reverse side if necessary and identify by block number)

Nuclear Weapons, Fireball

20. ABSTRACT (Continue on reverse side if necessary and identify by block number)

A model is developed which treats the growth of a fireball from an atmospheric nuclear detonation up to the point of hydrodynamic separation. The radius of the fireball and the partition of energy among streaming radiation, material temperature, and thermal radiation are predicted as a function of time. A simplified model is developed which applies when equilibrium between material temperature and thermal radiation temperature is reached.

Numerical results are calculated for various yields and yield pulse shapes.

DD FORM 1 JAN 73 1473 EDITION OF 1 NOV 65 IS OBSOLETE

UNCLASSIFIED

SECURITY CLASSIFICATION OF THIS PAGE (When Data Entered)

These results are compared to those predicted by the model previously developed by G. C. Pomraning.

The model developed here predicts reasonable numerical results and physically reasonable time dependences. It does not entail integrations over retarded time or the use of moments of radiation transport equations. It engenders an intuitive understanding of the fireball growth process and was developed for pedagogical use.